Long-Range Forecasting and Climate Research

The impact of El Niño on an ensemble of extended-range forecasts

by

J.A. Owen and T.N. Palmer

LRFC 10 **December 1986**

JC

THE IMPACT OF EL NIÑO ON AN ENSEMBLE OF EXTENDED-RANGE FORECASTS

by

J.A. OWEN AND T.N. PALMER*
LRFC 10

Met O 13 (Synoptic Climatology)
Meteorological Office
London Road
Bracknell
Berkshire
RG12 2SZ

December 1986

*Present address: European Centre for Medium Range Weather Forecasts, Reading, UK.

Abstract

Two ensembles of 90-day forecasts for 1982-83 have been made with the UK Meteorological Office 11-layer atmospheric general circulation model. Each ensemble comprised three integrations initialised one day apart, using analyses from December 1982. The first ensemble used observed SSTs and the second used climatological SSTs. Our objectives were to compare the skill of the two ensembles and to compare the results with a longer climate sensitivity experiment.

The skill of the forecasts for 10-, 30- and 90-day means was assessed using root-mean-square wind errors at 200 mb. In the tropics, the skill was improved with observed SSTs on all timescales. In the extratropics, the skill was improved on the 30-day timescale except at the initial stages of the forecasts, and the skill was also improved for 90-day means. On the 10-day timescale, however, the improvement was not consistent, and there were periods in which the errors were larger with SSTs. The response of the model to the observed SSTs was found to be similar to that of a 540-day perpetual January integration with the winter mean SST anomaly for 1982-83.

1. Introduction

The impact of the sea surface temperature (SST) anomalies on the atmospheric general circulation, particularly during an El Nino event, has been studied by a number of modelling groups around the world (see, for example, the papers in Nihoul, 1985). Typically, these 'climate sensitivity' (CS) experiments are run over several annual cycles, or for several hundred days in perpetual solstice mode. At least for those models which do not have serious systematic biases, results show that El Nino SST anomalies can force a realistic and statistically significant time-averaged response around the entire tropical band, and over parts of North America and the North Pacific.

Results from studies of the impact of SSTs on the skill of numerical forecast (NF) experiments, on the other hand, are more equivocal. Miyakoda et al (1983), for example, found that the skill of some extended-range forecasts was not noticeably improved with observed rather than climatological SSTs. Mansfield (1986), however, studied forecasts from 5 different winters, and found that, in several cases, extratropical forecast skill was substantially improved with observed SSTs.

There are clearly difficulties in comparing results from these two types of experiments. Firstly NF and CS experiments have not been run with the same model and with comparable SSTs. Secondly, the response to SSTs in an NF experiment is dependent on initial conditions; in a CS experiment, the response is designed to be independent of the initial conditions. Related to this, NF and CS experiments involve different timescales. For example, Mansfield and Miyakoda (op cit) studied the skill of 15- and 20-day mean fields respectively, rather than the 60 day or longer mean fields of many CS experiments. Since the 'intrinsic variability' (with fixed SST) of an n-day average atmospheric field is a function of n, the statistical significance of the n-day mean atmospheric response to a given SST anomaly will also be a function of n.

In this paper the impact on extended-range forecasts of SST anomalies occurring during the exceptional El Nino of 1982/83 is studied. Specifically two time-lagged ensemble integrations, each of 90 days, initialised from consecutive 24 hour analyses, were run with observed and climatological SSTs.

Our objectives were twofold. Firstly, we wished to compare the skill of the two ensembles for different time mean fields. Related to this we wanted to assess the timescale on which the SST anomalies first had noticeable impact on the atmospheric flow. Secondly, we wished to compare these NF experiments with results from a CS experiment reported in Palmer and Mansfield (1986). This latter experiment had been run on essentially the same model as the forecasts, and in it the impact of the seasonal winter mean SST anomaly in the tropical Pacific for 1982/83 was assessed. In pursuing these objectives we have distinguished between the behaviour of the response in tropical and extratropical latitudes.

The experiments described here have also been run by a number of other modelling groups in a coordinated attempt to clarify the role of SST anomalies in extended range forecasts (W.M.O., 1986).

2. Preliminaries

i Description of the Model

The UK Meteorological Office 11-layer atmospheric GCM (Slingo, 1985) was used for these experiments. This is similar in many respects to the 5-layer GCM of Corby et al (1977), but with enhanced vertical resolution. The model uses sigma coordinates with irregularly spaced levels in the vertical, and a regular latitude-longitude grid in the horizontal. For the experiments described here the horizontal resolution was 2.5° x 3.75° (72 x 96 points).

The model is a global primitive equation finite-difference model with the following physical processes. The radiation is modelled by an interactive scheme (Slingo and Wilderspin, 1984) which allows feedback between humidity and cloud distributions. The boundary layer, which occupies the lowest three model layers, is described by the Clarke scheme (Clarke, 1970). Large scale precipitation is formed when the relative humidity exceeds 100%, while convection is modelled by a scheme which treats both unsaturated and saturated convection (Lyne and Rowntree, 1976).

The mean orographic heights used in the operational model of the European Centre for Medium-Range Weather Forecasts (ECMWF) were interpolated from their 1.875° x 1.875° grid and used in these experiments. A gravity-wave drag parametrization scheme (Palmer et al., 1986) was incorporated, which reduces the excessive westerly flow in the northern mid-latitudes in winter.

The appropriate part of the annual radiation cycle was used, and SSTs and ozone amounts were regularly updated. The SSTs that were used are described in the next section and were updated every 5 days. Climatological ozone concentrations were udated every 30 days.

ii Description of the Experiments

In all, six experiments were run. Half of these used climatological SSTs (Alexander and Mobley, 1976) while the other three experiments used the observed SSTs between December 1982 and March 1983, obtained from Climate Analysis Center (Washington) analyses. The SSTs were linearly interpolated from monthly to five-day means.

ECMWF initialised analyses for the 15th, 16th and 17th of December 1982 at 12Z were used for initial conditions. The two experiments starting from the 15th December were run for two days preliminary to the main part of the integration, while those from the 16th were run for one preliminary day. Each experiment was then run for 90 days, thus producing two ensembles of three experiments, which will be referred to as OBS (with observed SSTs) and CLIM (with climatological SSTs).

The forecast experiments with observed SSTs were somewhat idealised since it is assumed that the SSTs for the whole period are known in advance. Therefore the results represent the potential impact of SST anomalies in a situation where these anomalies could be predicted, for example by a coupled ocean-atmosphere model (see, for example, Cane and Zebiak (1985)).

iii Some Observations

During the period the experiments covered, the El Nino/Southern Oscillation (ENSO) event was at its strongest. This particular ENSO event was the strongest that has been recorded, and it produced some remarkable climatic anomalies (Quiroz, 1983).

Of particular interest to us are the SST anomalies associated with this event. The SST anomalies for December 1982 are shown in Fig. 1. As a result of these anomalies, the SST maximum which is normally to be found in the equatorial west Pacific has been replaced by two maxima in the Central Pacific. The pattern of Fig. 1 persisted from December 1982 to March 1983, although the magnitude of the anomaly decreased during 1983.

Associated with these SST anomalies there were unusually large negative anomalies of outgoing long-wave radiation in the Central Pacific. The region of maximum negative anomaly moved eastwards and intensified during the period of the ENSO event, reaching a maximum value at around 140°W in February 1983 (Quiroz, 1983).

The effects were not confined to the tropical regions. In the north-east Pacific there were exceptionally low mean values of mean sea level pressure and geopotential height at all levels in the troposphere. This had major consequences for the weather of North America, giving many places their warmest winter on record, while others had excessive precipitation and flooding.

A diagnostic which we shall make particular use of for displaying model results is the 200 mb streamfunction. The mean 200 mb streamfunction anomaly for the 90-day period of the forecast (18th December to 17th March) is given in Fig. 2. This was obtained from the winds of the mean ECMWF analysis and the mean winter climatology of Oort (1983). It shows a pair of anticyclonic anomalies straddling the equator in the central Pacific with the associated anomalous easterly flow, together with the cyclonic anomaly in the north-east Pacific referred to above. In addition, over North America, we note an oppositely oriented high/low dipole with anomalous easterly flow over much of the continent.

3. Results of the Forecast Experiments

i The Climatological response

We first compare the response of the model using climatological SST's with the climatological circulation statistics of Oort (1983). The 200 mb streamfunction for days 1-90 of CLIM is plotted in Fig. 3(a). The difference between this and climatology (OORT) for the December/January/February period is shown in Fig. 3(b). The individual integrations (not shown) show similar patterns. The most notable bias is an overestimation of the strength of the westerly winds over Europe and Asia (by up to 6 ms^{-1} over south-west Europe). Also evident is a belt of anomalous easterly flow over the tropical regions of South America, the Atlantic Ocean and Africa. It should be noted, however, that these biases are sensitive to the climatology used. For instance, when a shorter Meteorological Office climatology is used, the westerly anomalies over Europe are weaker, but other anomalies are stronger.

For precipitation we concentrate on the region of the Pacific Ocean north of 30°S. The distribution of total precipitation for days 1-90 of CLIM is shown in Fig. 4. Since the climatological precipitation distribution over the Pacific Ocean is not very well known even on a yearly basis, let alone a seasonal basis, the difference between CLIM and the real climatology is not plotted. However, comparison with available climatologies (e.g. Dorman and Bourke (1979), Jaeger (1976)) indicates that the main features of the precipitation pattern are well represented.

ii Response to the observed SST's

In this section we present results of the difference between OBS and CLIM. In Fig. 5 the 200 mb streamfunction difference for days 1-30 is plotted. Over the central equatorial Pacific there are anomalous easterlies, associated with a weakening of the Pacific Walker cell (the normal equatorial circulation with ascent over the west Pacific, high level westerly flow and descent over the east Pacific). Elsewhere in the tropics and also in mid-latitudes the anomalous non-divergent wind is, in general, westerly. Also, a weak Pacific North America (PNA) pattern (Wallace and Gutzler, 1981) is present, similar to the observed anomalies (see Fig. 2).

In order to assess the statistical significance of this result, we must consider the differences between the individual integrations comprising each ensemble. These are plotted in Fig. 6 and show a consistent pattern in the eastern Pacific ocean, although there are marked differences elsewhere. We wish to calculate the Student's t-statistic for the difference between OBS and CLIM, but the streamfunction is unsuitable for this purpose since it is defined only up to an arbitrary constant. We therefore use the differences of 200 mb geopotential height instead. Assuming that the three integrations within each ensemble are independent members of a normal distribution of possible forecasts from the given initial conditions then we can say the following: if t is greater than 2.1 then OBS is significantly greater than CLIM at the 10% level and vice-versa if t is less than -2.1. The areas for which t is greater than 2.1 are dotted in Fig. 5. These results are discussed below.

Fig. 7 shows the ensemble mean 200 mb velocity potential for OBS - CLIM. The outstanding feature is the large negative anomaly over the central/eastern equatorial Pacific, associated with anomalous divergence over the area of positive SST anomalies. The corresponding precipitation difference for the Pacific is shown in Fig. 8. The dotted areas indicate positive anomalies of greater than 1 mm/day and these are in general positioned over the areas of maximum SST anomalies, i.e. along the equator with maxima at 135°W and 160°E. Either side of this band of excess precipitation are substantial areas of precipitation deficit which are probably associated with an intensification of the Hadley circulation. There is also an area of precipitation deficit over the equatorial west Pacific at 135°E associated with anomalous descent and cooler than normal SST's. It appears however that the absolute values of the precipitation anomalies are somewhat high, even though the pattern may be reasonable.

We next consider the ensemble-mean 200 mb streamfunction differences between OBS and CLIM for days 31-60 and 61-90. These patterns, together with the areas of significant difference of the 200 mb height, are shown in Fig. 9. The PNA pattern is stronger in days 31-60 than 1-30, but is not so evident in days 61-90. There is a good deal of persistence of the global difference pattern through the three 30-day periods, indicating a consistent response to the persistent SST anomalies.

The results of the t-tests show that the difference between OBS and CLIM is highly significant over the tropics for the whole 90-day period. This is due mainly to the small variance of the 200 mb height in that region. In the extratropics the difference is significant only over very limited regions. Although the 200 mb height difference increases as the integration proceeds, the significance does not, since the variance within each ensemble also increases. There are a few areas where this is not true: for instance, over the north-east Pacific the significance of the difference is greater for days 31-60 than for days 1-30. It could be argued, however, that even the difference here is not statistically significant since on average one would expect 10% of any area to show a significant difference at the 10% level. The fact that the response in this area is consistent over the three 30-day periods suggests that this is not the case (see the conclusions for further discussion).

The t-test has also been carried out for the 90-day mean difference 200 mb height. Again the largest area of significant difference in the extra-tropics is over the north-east Pacific. In general, over this area, the average value of the t-statistic for the 30-day mean fields is smaller than the corresponding value for the 90-day mean field.

iii Skill of the forecasts

We now compare the response of the model with the real atmosphere (REAL). Fig. 10 shows the 200 mb streamfunction difference between OBS and CLIM for days 1-90. This should be compared with Fig. 2 which shows the atmospheric anomalies (REAL-OORT) for the same period. Over the Pacific Ocean the anomaly patterns are similar, but the magnitudes are slightly larger in the real atmosphere. Elsewhere over the tropics the observed anomalies are weaker, but still westerly as in the model. It thus seems that, irrespective of the skill of the model, the anomalies forced in the mdoel by the SST anomalies correspond fairly well to observations.

In Figs. 11 and 12 the 200 mb streamfunction errors of the two ensembles (i.e. OBS - REAL and CLIM - REAL) are plotted for days 1-30 and 31-60. In the tropics it is clear that in both periods there is an improvement with the observed SST's, with substantial weakening of gradients. In the extra-tropics there is no discernible improvement in days 1-30, but by days 31-60 the improvement is quite noticeable, especially in the northern hemisphere. An improvement is also evident in days 61-90 (not shown).

In order to assess the impact of SST's objectively, we have calculated root-mean-square (RMS) errors of 500 mb height and winds at 850 mb and 200 mb in three regions, the "northern hemisphere" (30°N-90°N), the tropics (30°S-30°N) and the "southern hemisphere" (30°-90°S). Although our main aim is to see the difference in RMS error between OBS and CLIM, we have also, for reference, calculated the RMS error for persistence (PERS). To do this we have used the mean of the ECMWF analyses for the ten days prior to the 18 December 1982 (day 1 of the integrations).

Results for the RMS of the magnitude of the 200 mb vector wind error are shown in Fig. 13. The results for the 850 mb wind and 500 mb height are similar. The values plotted are the RMS errors for 30-day mean fields (days 1-30, 11-40, 21-50, etc) for OBS, CLIM and PERS. In the tropics the reduction in RMS error with observed SST's is substantial and continues throughout the forecast. In the extra-tropics the reduction is smaller, but still evident in all but the first 30-day period.

RMS errors over a limited Pacific/North American region (70°-160°W, 20°-60°N) have been calculated. While there is more variability of the RMS errors from one period to the next because of the limited area, the RMS error of OBS is still lower than that of CLIM in every 30-day period up to days 31-60. This may not be true in other regions where the difference between OBS and CLIM is not so significant.

The corresponding RMS errors for 10-day means have also been calculated. These are shown in Fig. 14. Again the improvement with observed SST's in the tropics is immediate and substantial. In the extratropics the observed SST's generally gave rise to lower errors in the first half of the forecasts, but not thereafter. Finally, the 90-day mean RMS errors have been calculated and are indicated at the right-hand side of Fig. 14. In each case they show smaller errors with observed SSTs.

4. Conclusions

In this paper we have described results from two ensembles of 90-day integrations for the winter 1982/83. Each ensemble comprised three integrations initialised one day apart. The first of the two ensembles was integrated with observed SSTs, the second with climatological SSTs. Our objectives were to compare the skill of the two ensembles for different time-mean fields, and to compare results with a longer climate sensitivity experiment with observed 1982/83 SST anomalies.

The skill of the model was assessed using 200 mb RMS wind speed errors for 10-day, 30-day and 90-day mean fields. It was shown that, in the tropics, forecast skill was consistently improved with observed SSTs, on all timescales. In the extratropics, skill was generally, but not consistently improved on the 10-day timescale. On the 30-day timescale there was no improvement in the first period, but consistent improvement thereafter. On the seasonal timescale, the RMS error was significantly smaller in both northern and southern hemispheres.

These results are in agreement with conclusions made in Palmer (1987), that SST anomalies should have a consistent impact on forecast skill in the tropics on the monthly timescales but a longer averaging period may be required in the extratropics.

In Palmer and Mansfield (1986) a 540-day perpetual January integration was made, testing the model response to the winter seasonal mean SST anomaly for 1982/83. The 250 mb geopotential height response is shown in Fig. 15(a) (see Palmer and Mansfield, op cit, for details). The correspondence between the response over the PNA area in Fig. 15(a) and the difference fields (Figs. 5 and 9) in teh forecast experiment is encouraging. In particular the similarity between Fig. 15(a) and Fig. 5 for the day 1-30 ensemble-mean difference field suggests that although the extra-tropical day 1-30 difference field over the PNA area is not formally statistically significant, it is not likely to be spurious. Also encouraging is the fact that the pattern of t-statistic for the day 1-30 and day 31-60 difference fields is quite similar to the t-statistic calculated from the 6-pairs of non-overlapping 90-day mean fields comprising the 540-day mean difference field in climate sensitivity experiment (Fig. 15(b)).

References

Alexander, R.C. and Mobley, R.L., 1976, Monthly average sea-surface temperatures and ice-pack limits on a 1° global grid. Mon. Wea. Rev., 107, 896-910.

Cane, M.A. and Zebiak, S.E., 1985, A theory for El Nino and the Southern Oscillation. Science, 228, 1085-1087.

Clarke, R.H., 1970, Recommended methods for the treatment of the boundary layer in numerical models. Austr. Met. Mag., 18, 51-73.

Corby, G.A., Gilchrist, A. and Rowntree, P.R., 1977, United Kingdom Meteorological Office five-level general circulation model. Methods in Computational Physics, 17, 67-110.

Dorman, C.E. and Bourke, R.H., 1979, Precipitation over the Pacific Ocean, 30°S to 60°N, Mon. Wea. Rev., 107, 896-910.

Jaeger, L., 1976, Monatskarten des Niederschlags fur die ganze Erde. Berichte Dtsch. Wetterdienstes, 18 (139), 38 pp.

Lyne, W.H. and Rowntree, P.R., 1976, Development of a convective parametrization using GATE data. Met O 20 Technical Note II/70, Meteorological Office, Bracknell.

Mansfield, D.A., 1986, The skill of dynamical long-range forecasts, including the effect of sea surface temperature anomalies. Quart. J. Roy. Meteor. Soc., 112, 1145-1176.

Miyakoda, K., Gordon, T., Caverly, R., Stern, W., Sirutis, J. and Bourke, W., 1983, Simulation of a blocking event in January 1977. Mon. Wea. Rev., 111, 846-869.

Nihoul, J.C.J. (ed.), 1985, Coupled ocean-atmosphere models. Elsevier Oceanography Series Vol. 40, Elsevier Press, Amsterdam, 767 pp.

Oort, A.H., 1983, Global atmospheric circulation statistics, 1958-1973. NOAA Professional Paper 14, US Department of Commerce, Washington, 180 pp.

Palmer, T.N. and Mansfield, D.A., 1986, A study of wintertime circulation anomalies during past El Nino events, using a high resolution general circulation model. II Variability of the seasonal mean response. Quart. J. Roy. Meteor. Soc., 112, 639-660.

Palmer, T.N., Shutts, G. and Swinbank, R., 1986, Alleviation of a systematic westerly bias in general circulation and numerical weather prediction models through an orographic gravity wave drag parametrization. Quart. J. Roy. Meteor. Soc., 112, 1001-1040.

Palmer, T.N., 1987, Modelling low frequency variability of the atmosphere. In Variability of the atmosphere and the oceans (ed. H. Cattle), Royal Meteorological Society (to be published).

Quiroz, R.S., 1983, The climate of the "El Nino" winter of 1982-83 - season of extraordinary climatic anomalies. Mon. Wea. Rev., 111, 1685-1706.

Slingo, A. and Wilderspin, R.C., 1984, Development of a revised longwave radiation scheme for an atmospheric general circulation model. Dynamical Climatology Technical Note no. 14, Meteorological Office, Bracknell.

Slingo, A., 1985, Handbook of the Meteorological Office 11-layer atmospheric general circulation model, vol. 1. Dynamical Climatology Technical Note no. 29, Meteorological Office, Bracknell.

Wallace, J.M. and Gutzler, D.S., 1981, Teleconnections in the geopotential height field during the northern hemisphere winter. Mon. Wea. Rev., 109, 784-812.

W.M.O., 1986, Workshop on comparison of simulations by numerical models of the sensitivity of the atmospheric circulation to sea surface temperature anomalies. WCP 121, World Meteorological Organization, Geneva, 188 pp.

Figures

Fig. 1 Sea-surface temperature anomalies in °C for December 1982. The 0° contour has been omitted for clarity.

Fig. 2 200 mb streamfunction difference between the observed atmosphere from 18/12/82 to 17/3/83 and the December/January/February climatology of Oort. The contour interval is 6×10^6 $m^2 s^{-1}$

Fig. 3 (a) 200 mb streamfunction for days 1-90 of CLIM. The contour interval is 20×10^6 $m^2 s^{-1}$.

(b) 200 mb streamfunction difference between days 1-90 of CLIM and the December/January/February climatology of Oort. The contour interval is 6×10^6 $m^2 s^{-1}$.

Fig. 4 Total precipitation in the region 120°E-75°W, 30°S-60°N for days 1-90 of CLIM. Contours are at 0.5, 1.0, 2.0, 4.0, 8.0 and 16.0 mm day^{-1}.

Fig. 5 200 mb streamfunction difference between OBS and CLIM for days 1-30. The contour interval is 6×10^6 $m^2 s^{-1}$. The dotted areas are those for which the t-statistic of the 200 mb geopotential height difference between OBS and CLIM is greater than 2.1 in magnitude.

Fig. 6 (a) 200 mb streamfunction difference between days 1-30 of the integration with observed SST's which used initial conditions from 15/12/82 and days 1-30 of the corresponding integration with climatological SST's. The contour interval is 6×10^6 $m^2 s^{-1}$.

(b) As (a), but the difference between the integrations which used initial conditions from 16/12/82.

(c) As (a), but the difference between the integrations which used initial conditions from 17/12/82.

Fig. 7 200 mb velocity potential difference between OBS and CLIM for days 1-30. The contour interval is 2×10^6 $m^2 s^{-1}$.

Fig. 8 Total precipitation difference between OBS and CLIM for days 1-30 and the same region as Fig. 4. Contours are at $\pm$1, 2, 4, 8 and 16 mm day^{-1} The dotted region indicates values greater than 1 mm day^{-1}.

Fig. 9 (a) As Fig. 5, but days 31-60.

(b) As Fig. 5, but days 61-90.

Fig. 10 200 mb streamfunction difference between OBS and CLIM for days 1-90. The contour interval is 6×10^6 $m^2 s^{-1}$.

Fig. 11 (a) 200 mb streamfunction difference between days 1-30 of OBS and the corresponding period of the observed atmosphere. The contour interval is 6×10^6 $m^2 s^{-1}$.

(b) As (a), but with CLIM instead of OBS.

Fig. 12 (a) As Fig. 11(a), but for days 31-60.

(b) As Fig. 11(b), but for days 31-60.

Fig. 13 (a) 200 mb RMS wind vector errors in ms^{-1} for OBS, CLIM and PERS as a function of model date. Values are the 30-day mean errors for days 1-30, 11-40, ..., 61-90, averaged over the region from 30°N to 90°N, and plotted at the mid-point of each period.

(b) As (a), but for the region 30°S to 30°N.

(c) As (a), but for the region 90°S to 30°S.

Fig. 14 (a) As Fig. 13(a), except that the values are the 10-day mean errors for days 1-10, 11-20, ..., 81-90. The 90-day mean errors are shown at the right-hand side.

(b) As (a), but for the region 30°S to 30°N.

(c) As (a), but for the region 90°S to 30°S.

Fig. 15 (a) 250 mb geopotential height difference between a 540-day perpetual January integration with SST's averaged from December 1982 to February 1983 and a control integration with climatological SST's. The contour interval is 20 m.

(b) Values of the t-statistic corresponding to (a). The contour interval is 2.0.

(From Palmer and Mansfield (1986)).

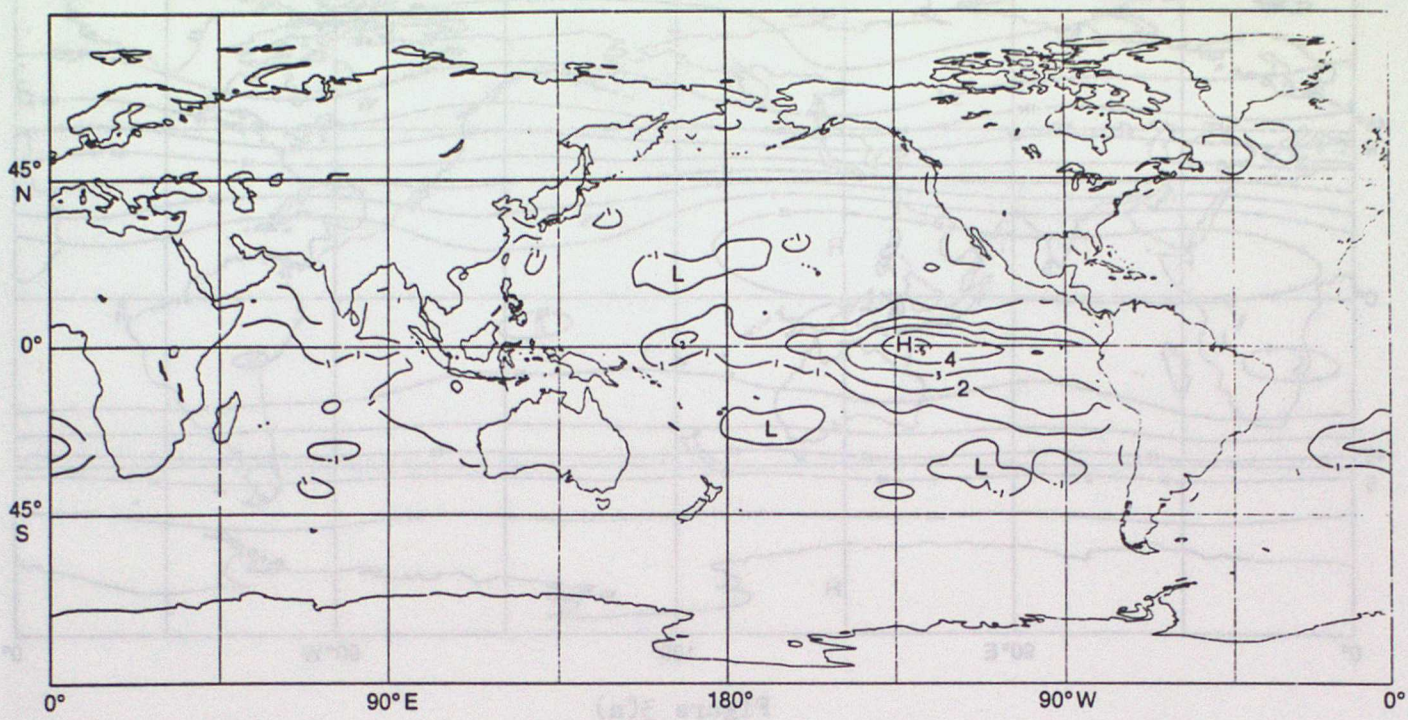

Figure 1

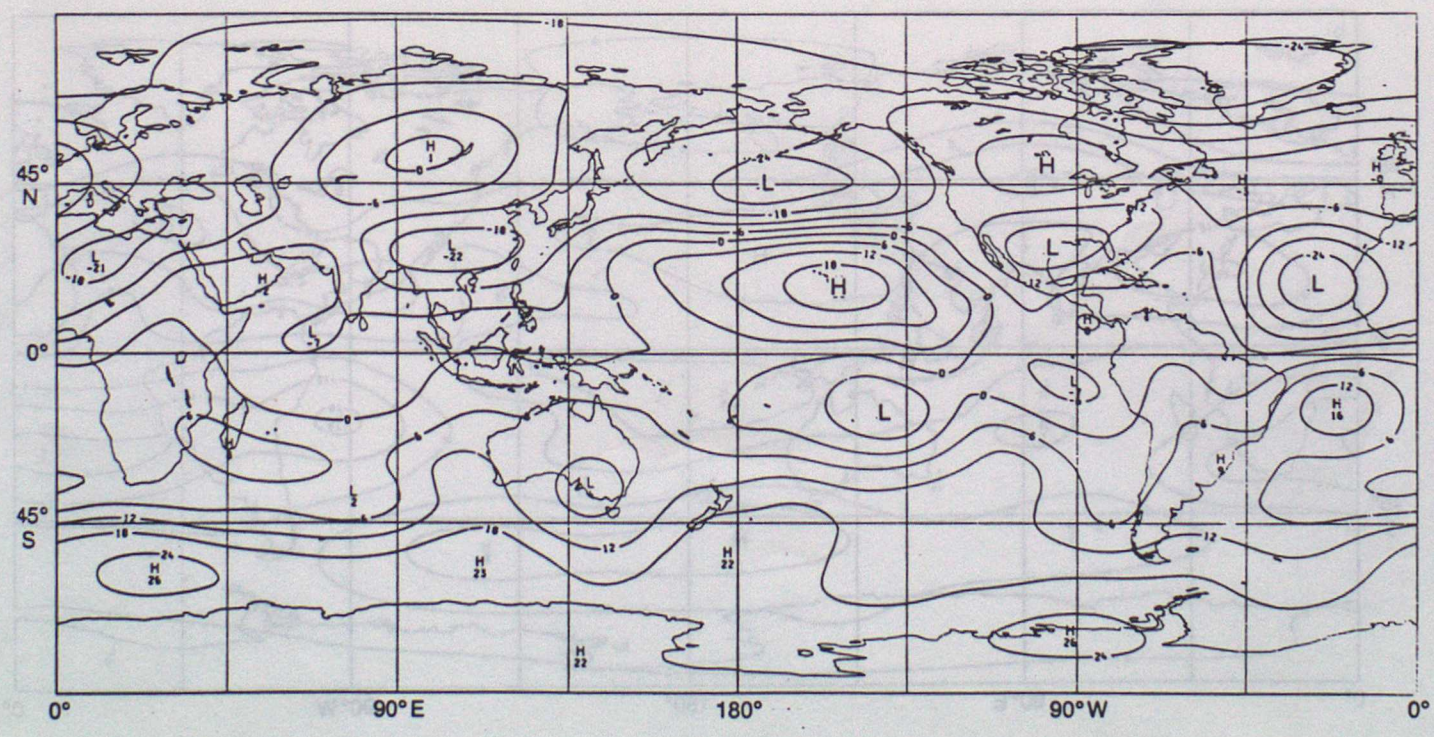

Figure 2

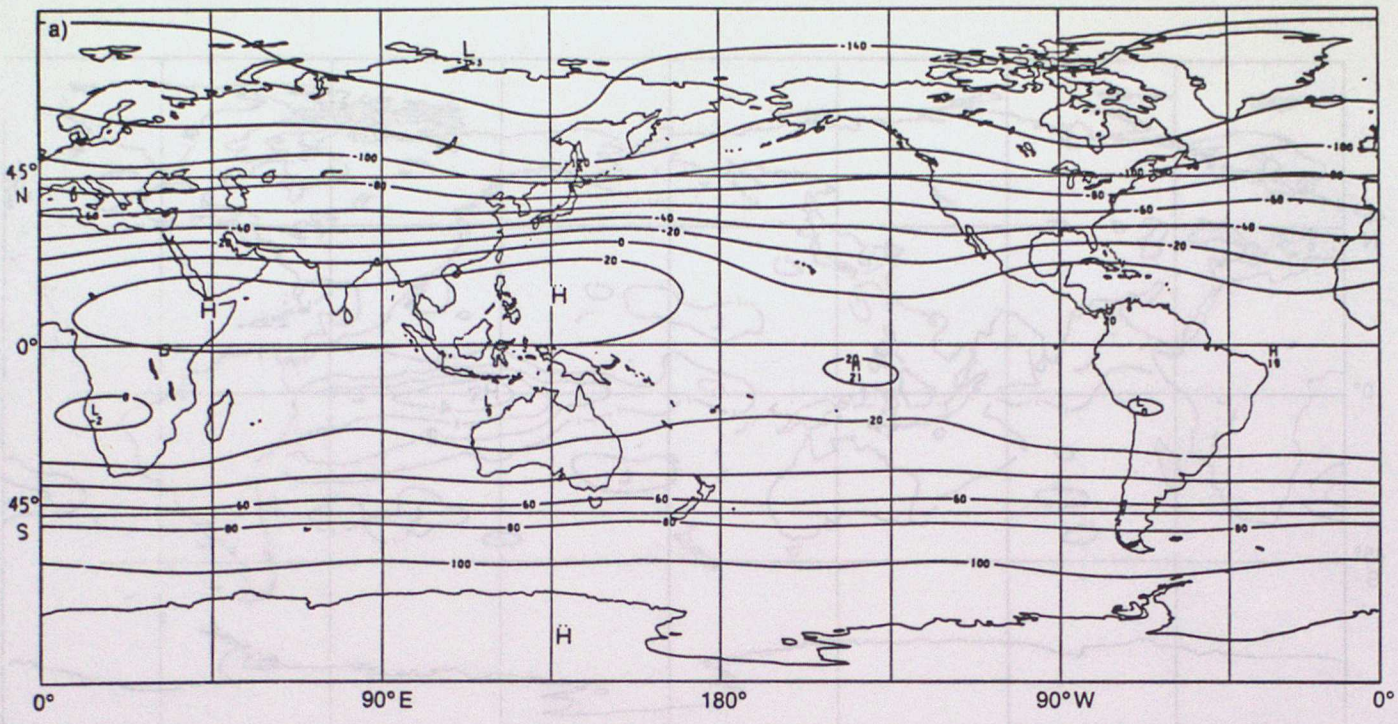

Figure 3(a)

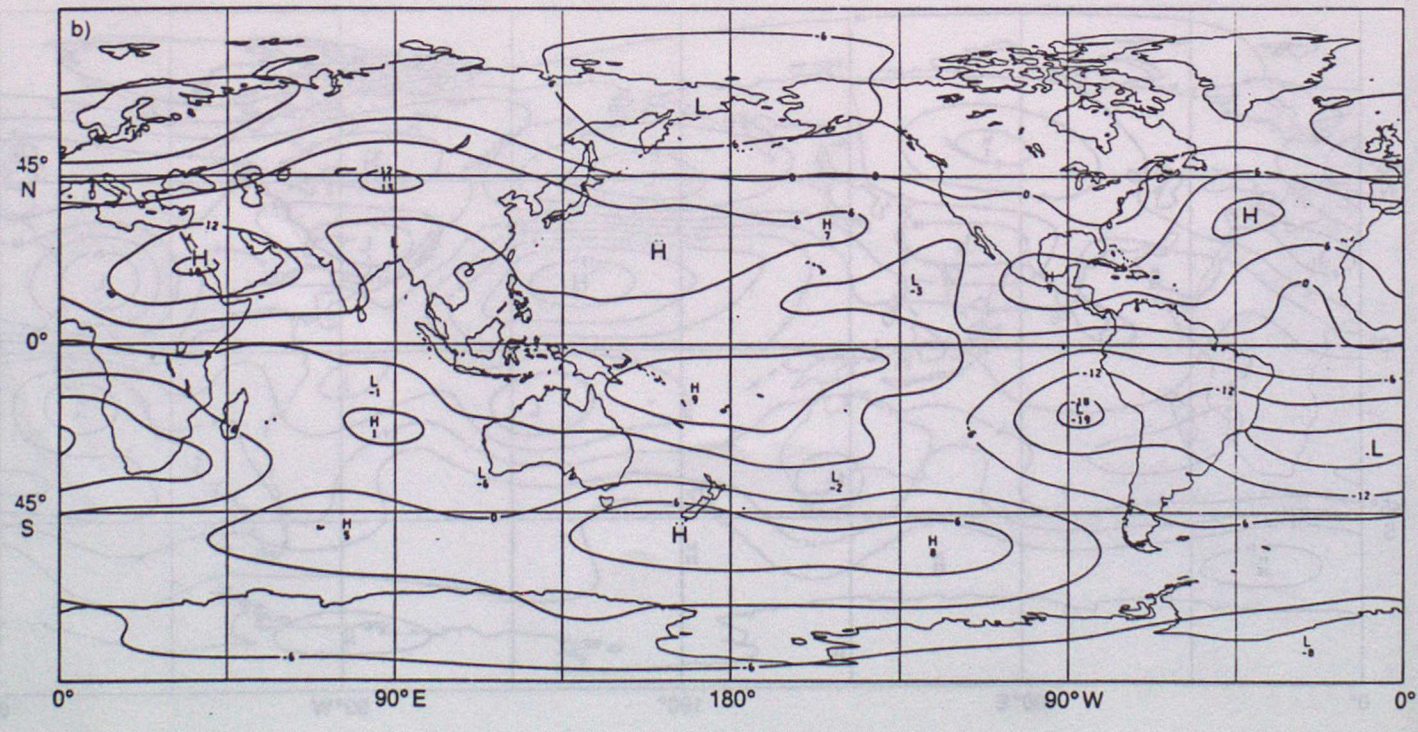

Figure 3(b)

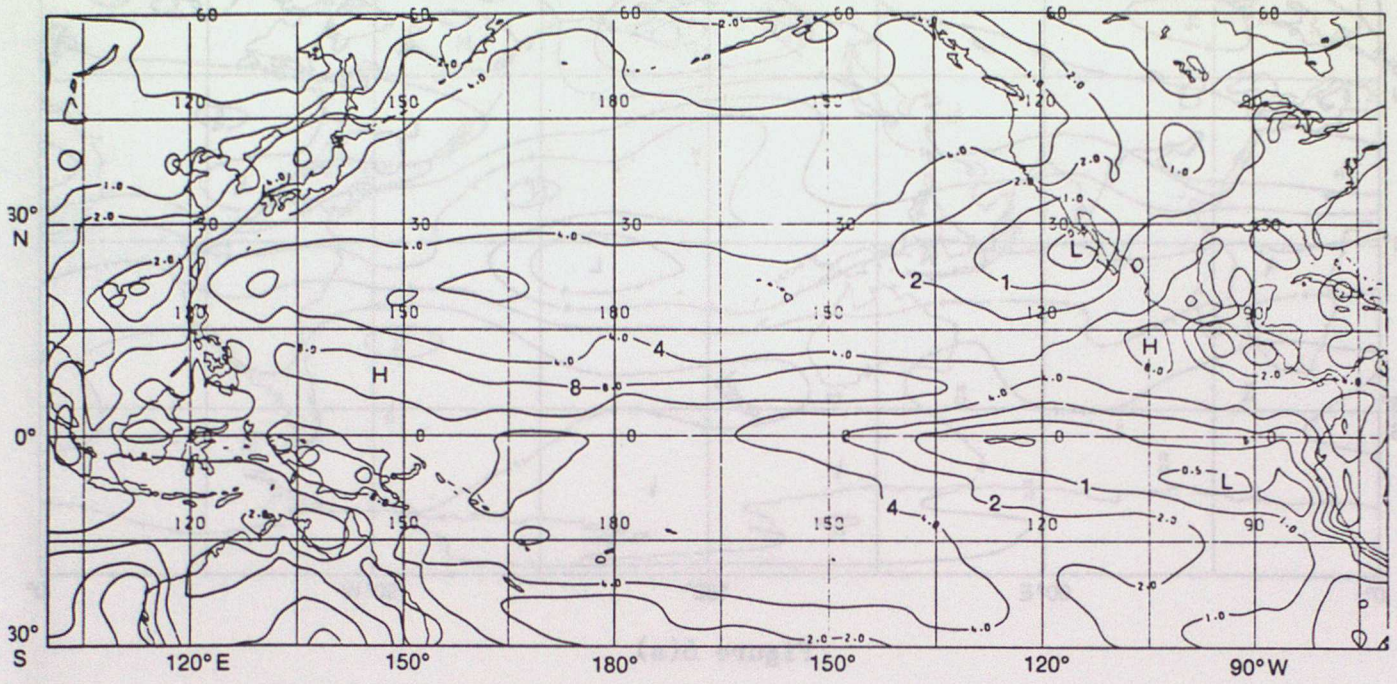

Figure 4

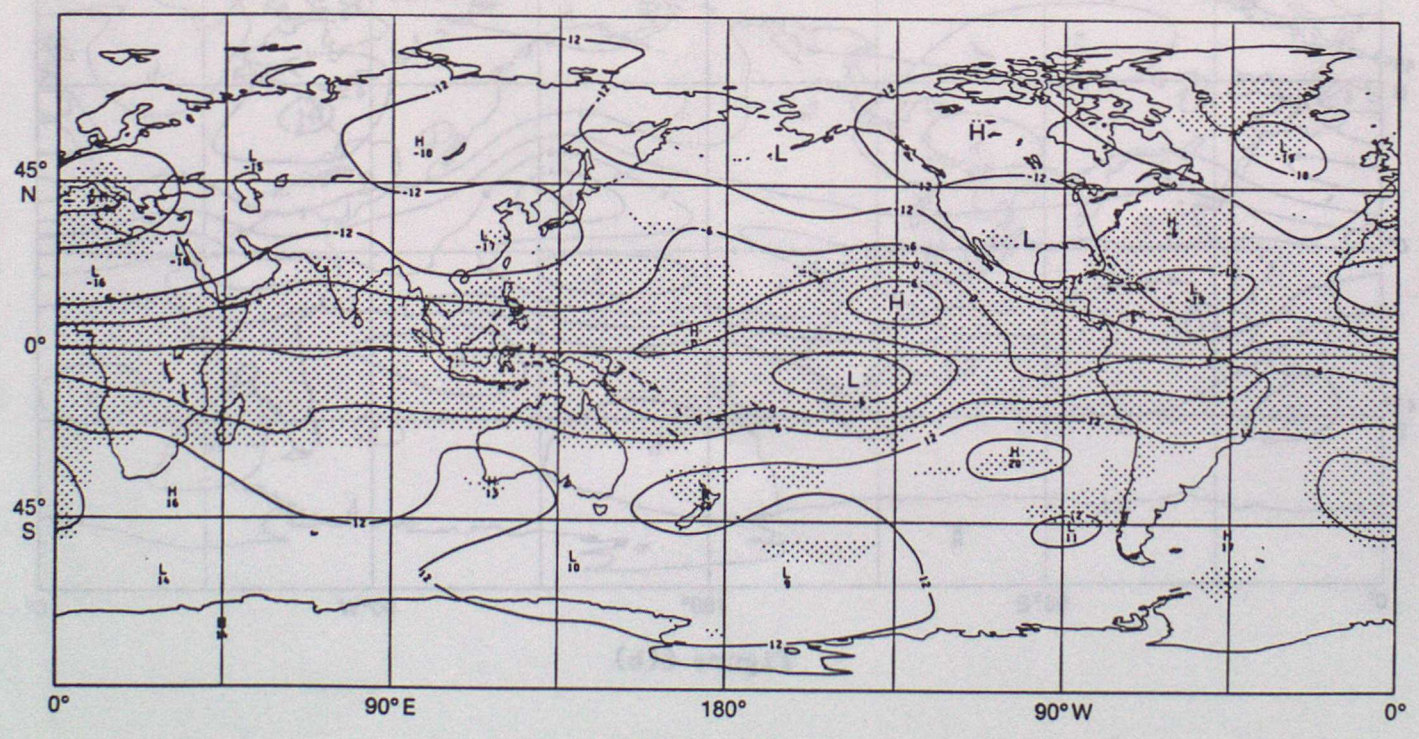

Figure 5

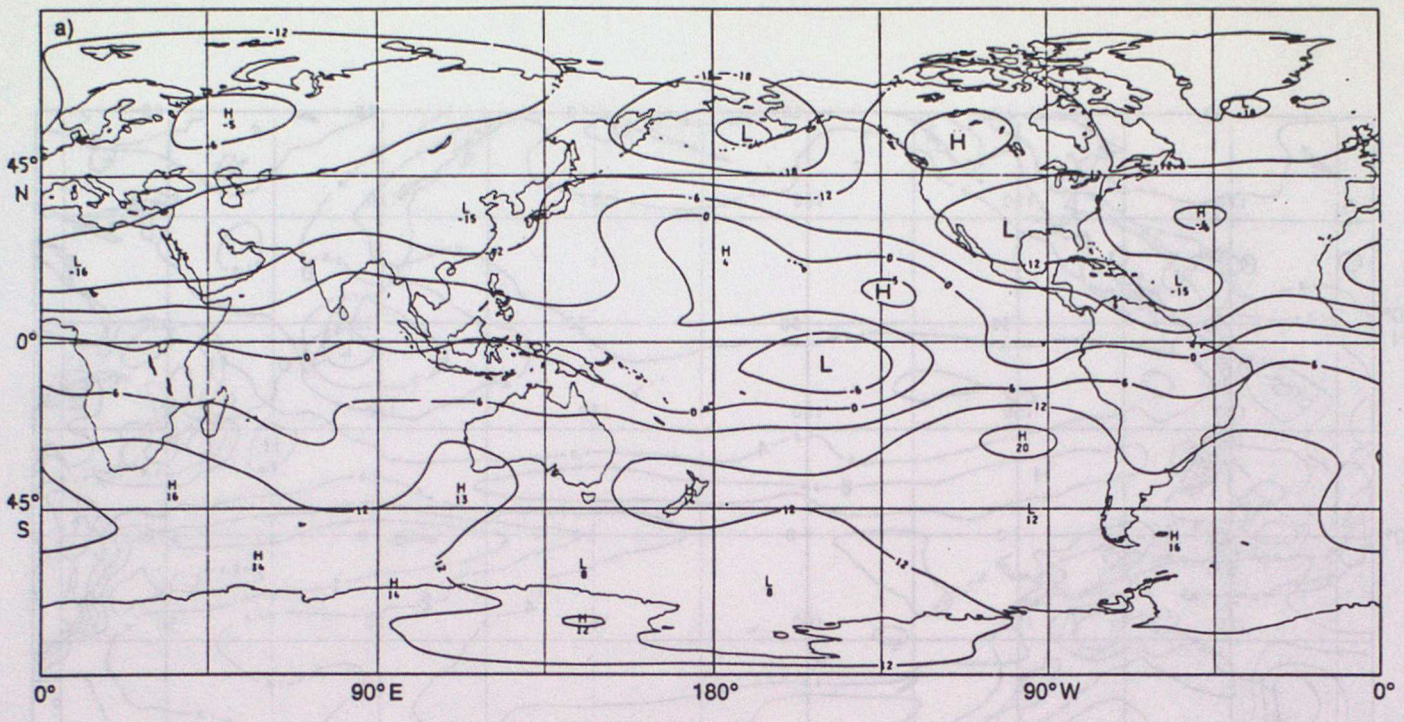

Figure 6(a)

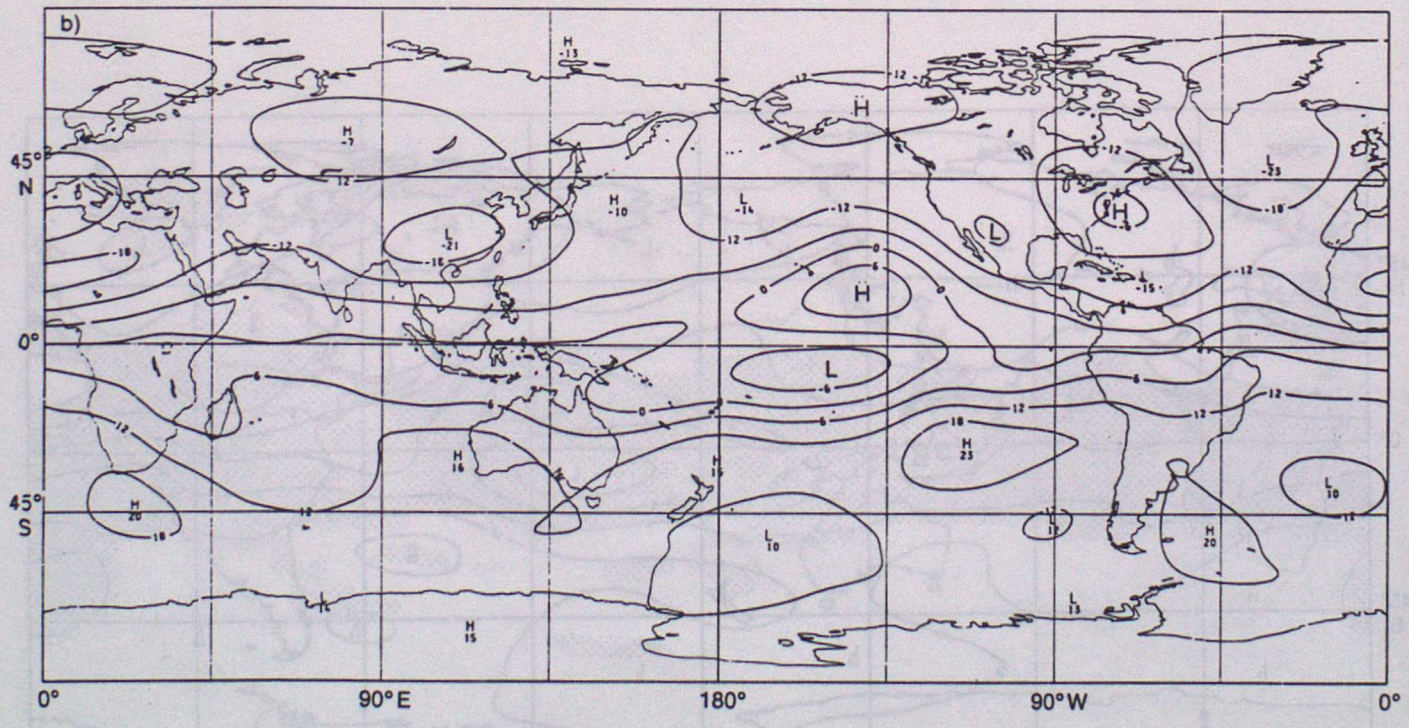

Figure 6(b)

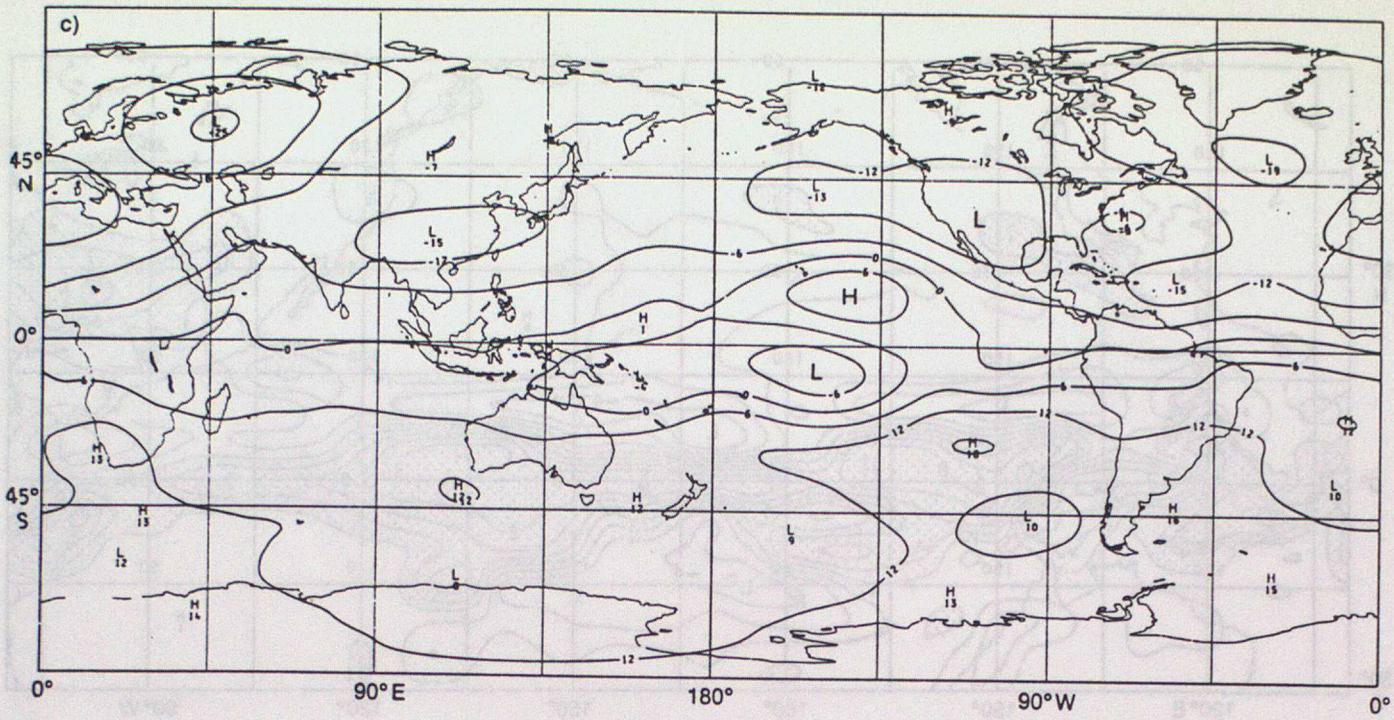

Figure 6(c)

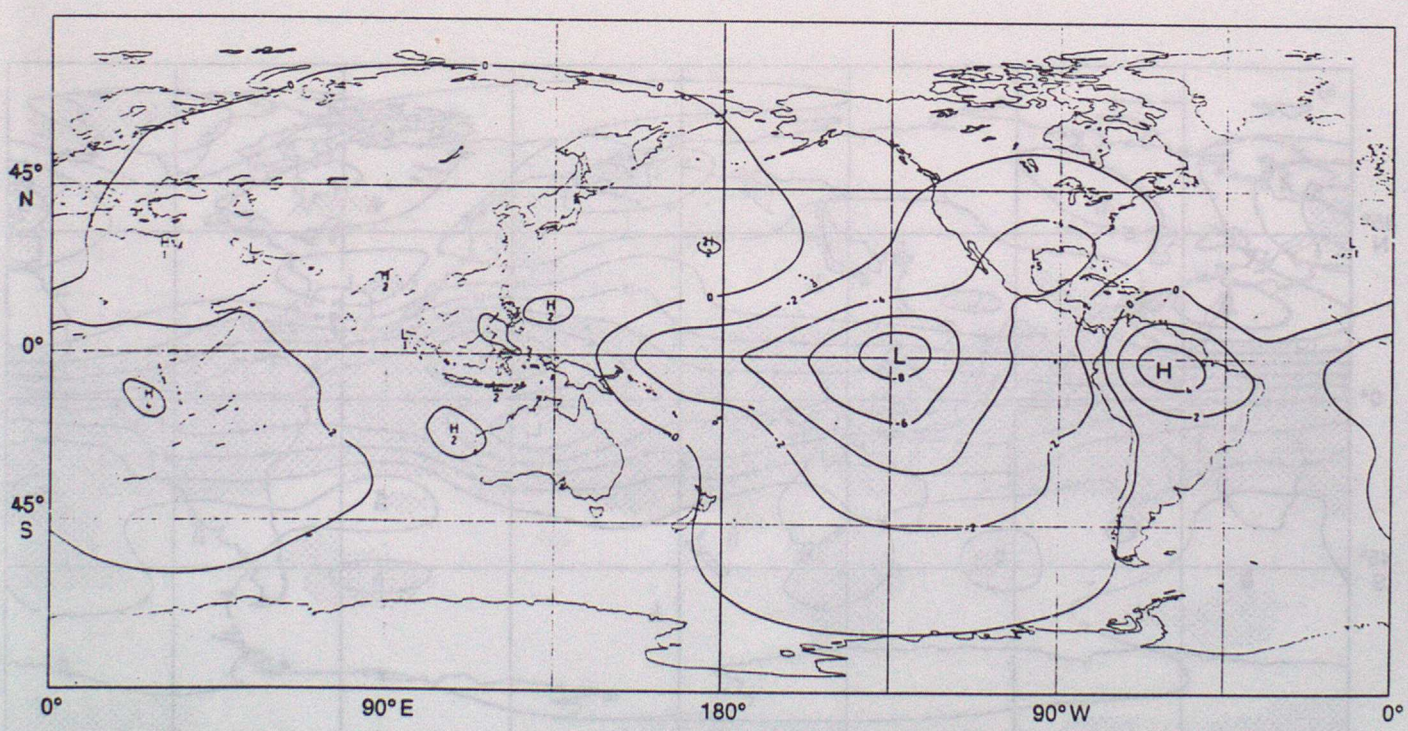

Figure 7

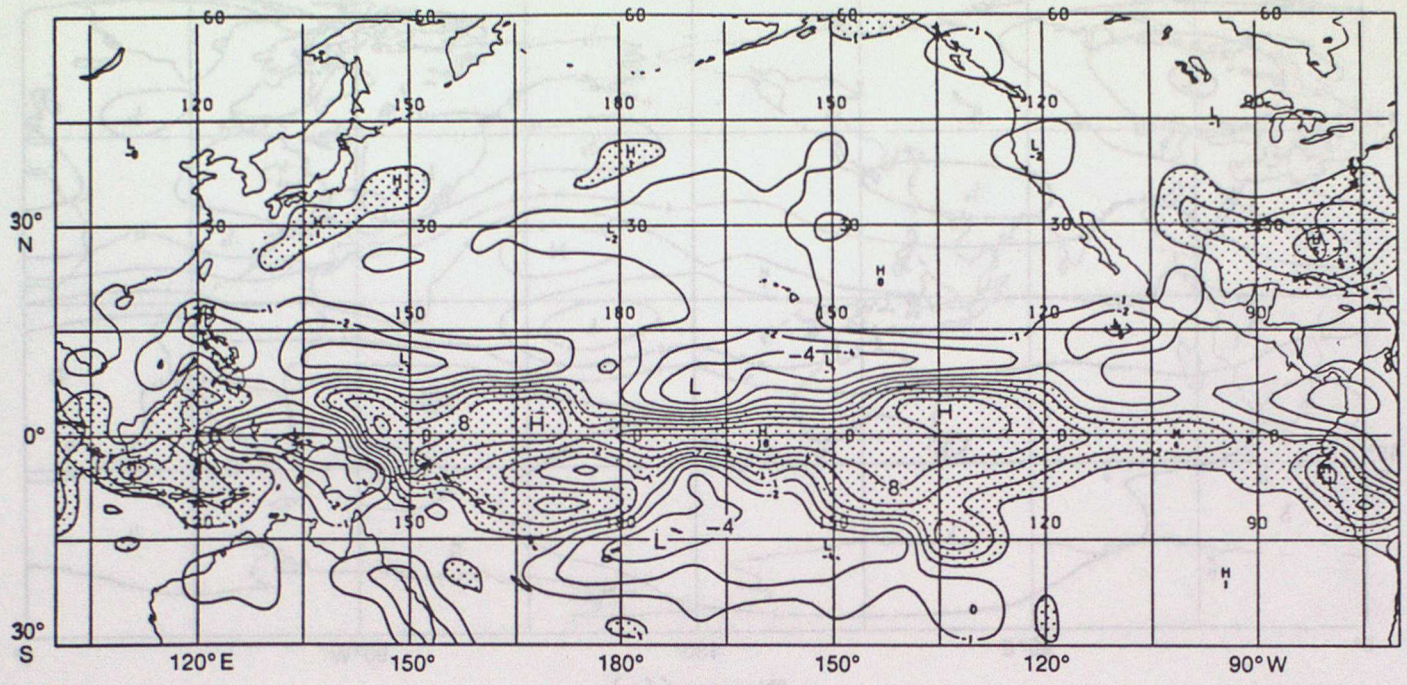

Figure 8

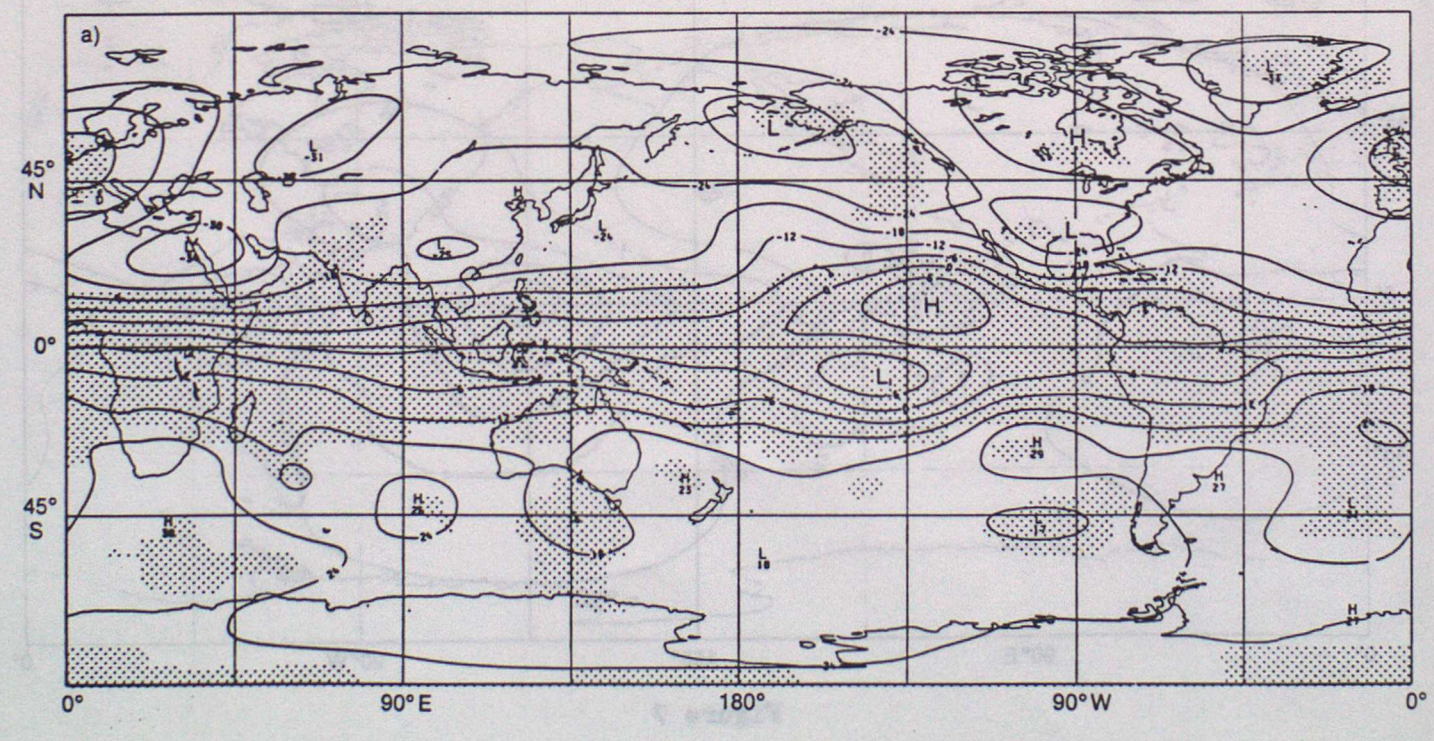

Figure 9(a)

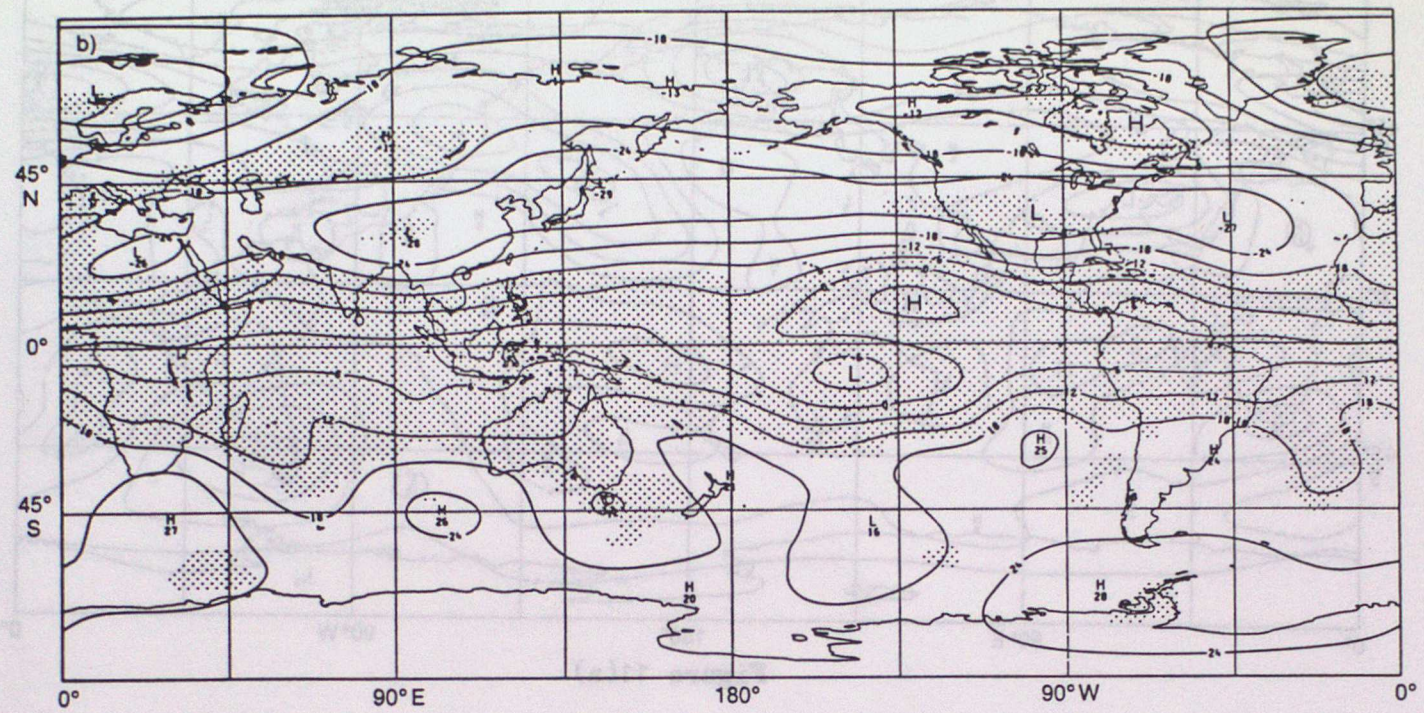

Figure 9(b)

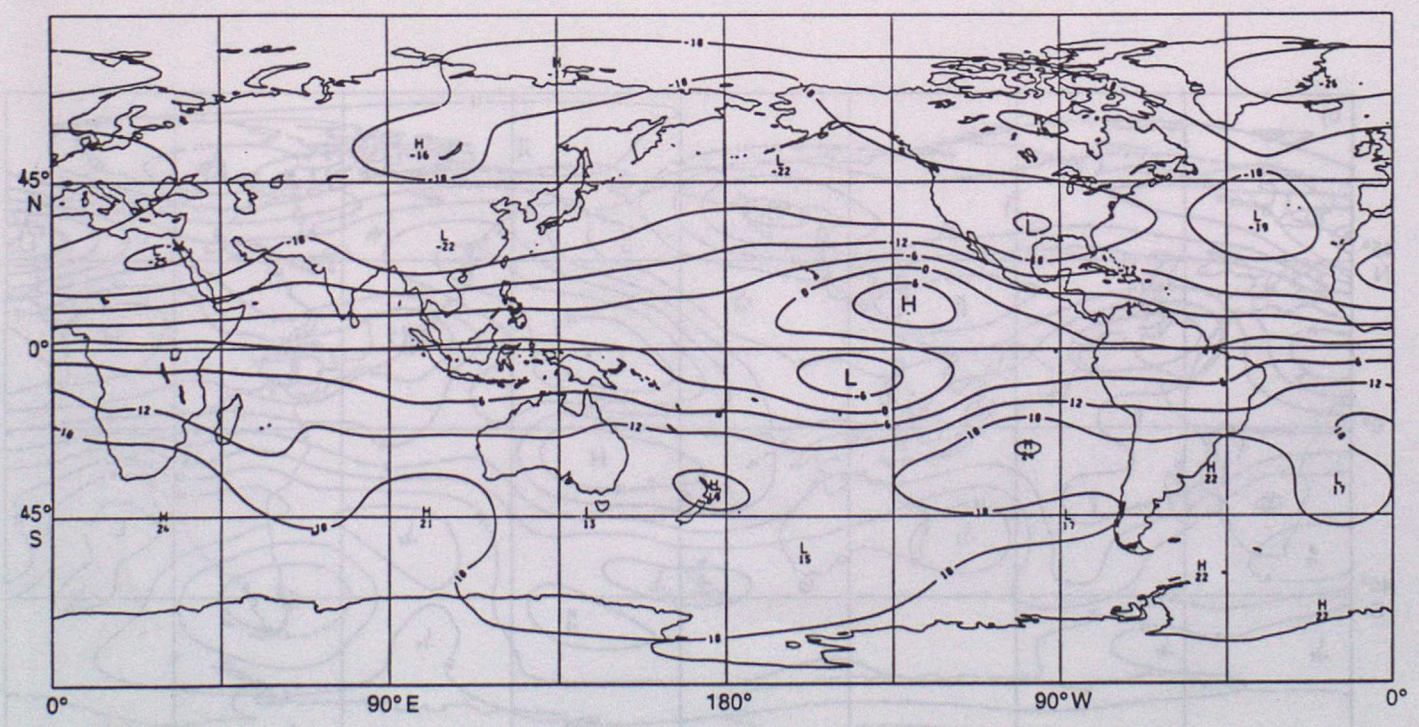

Figure 10

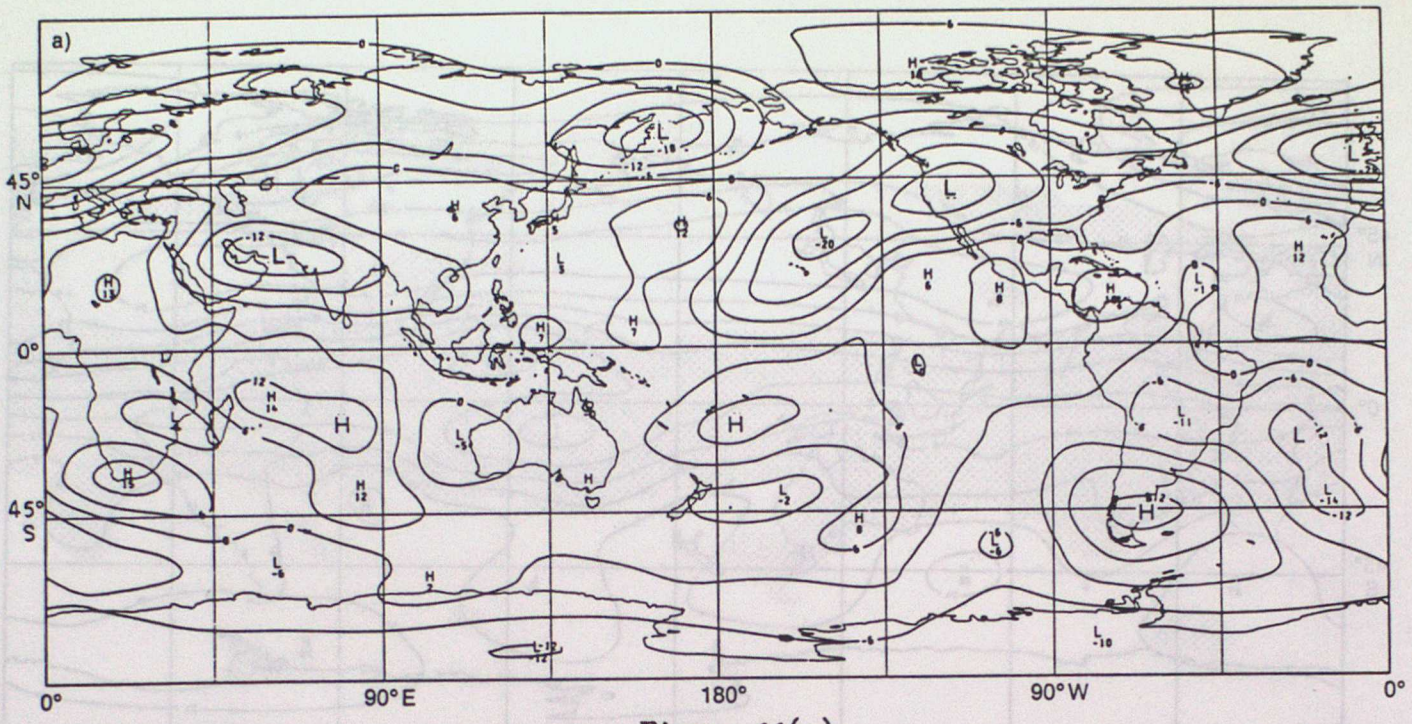

Figure 11(a)

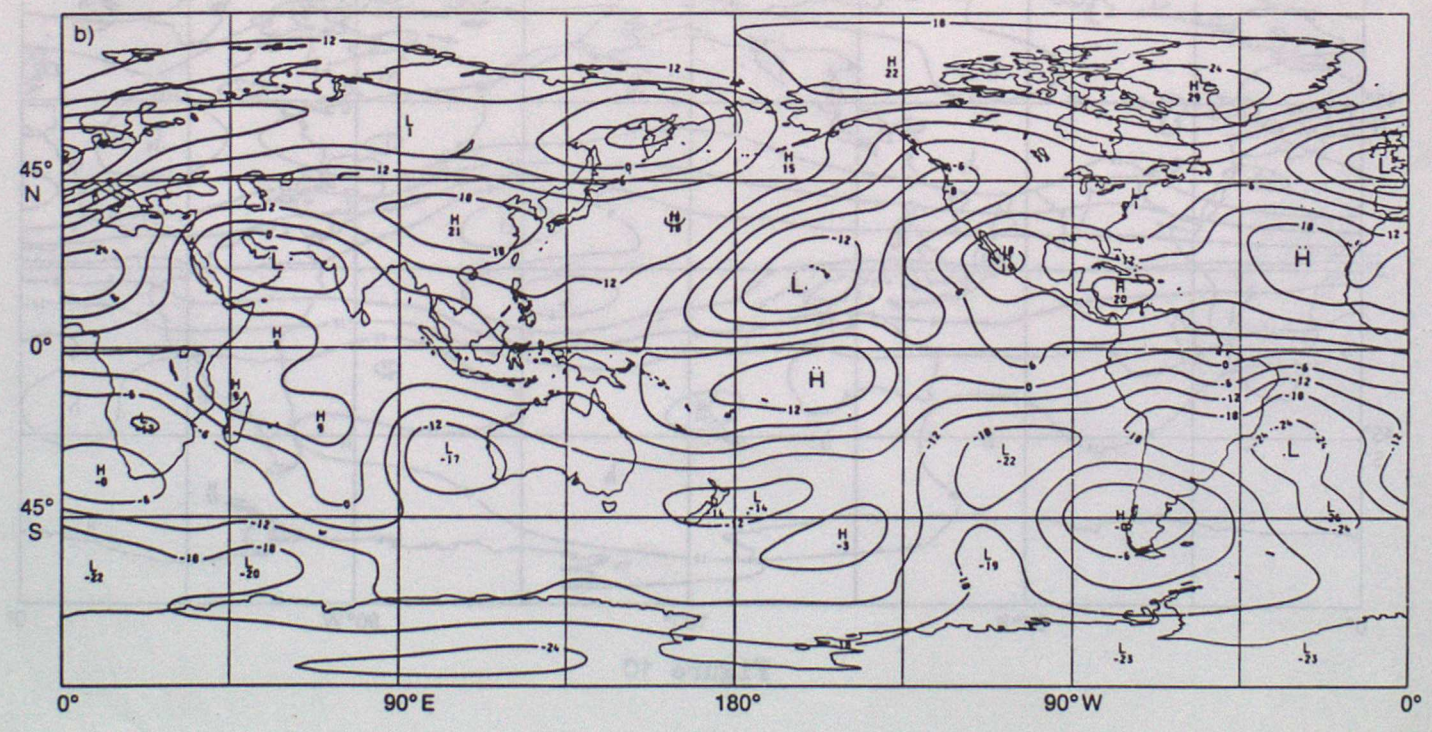

Figure 11(b)

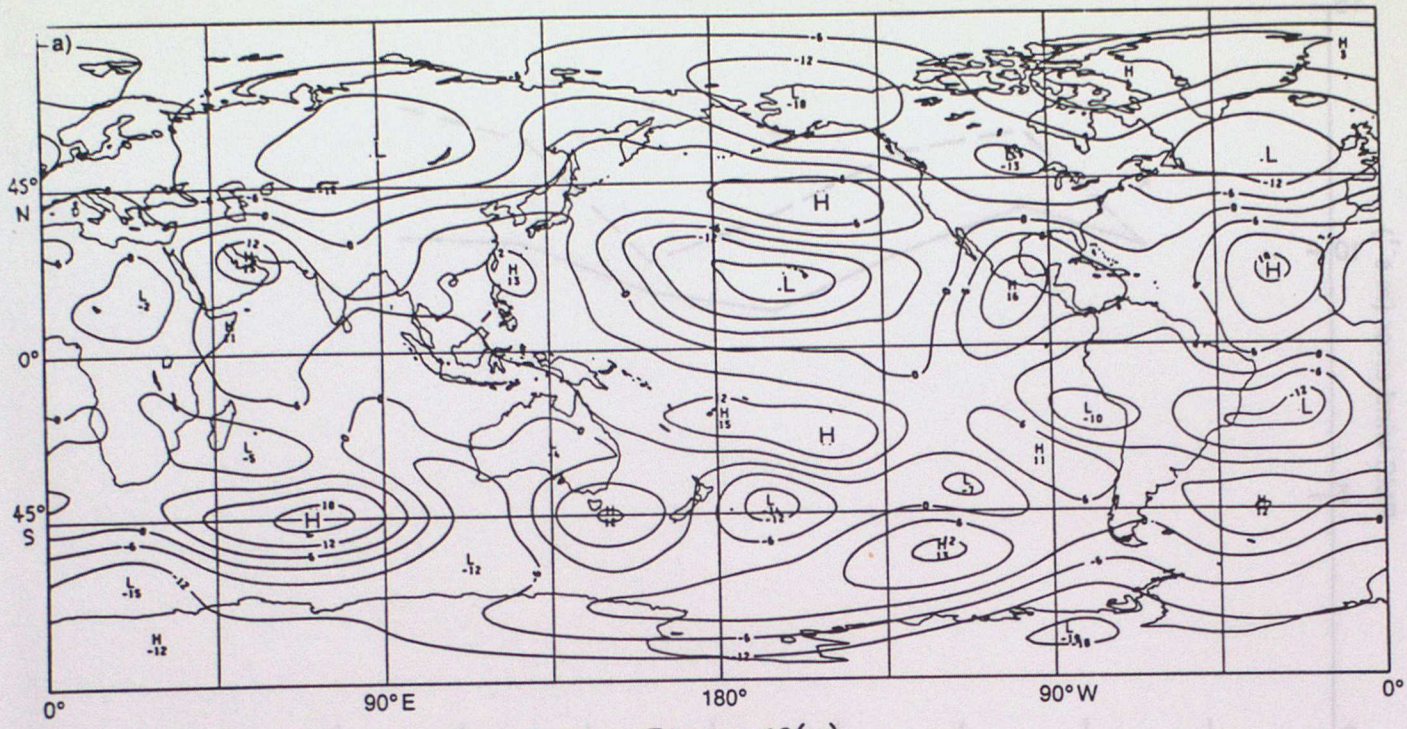

Figure 12(a)

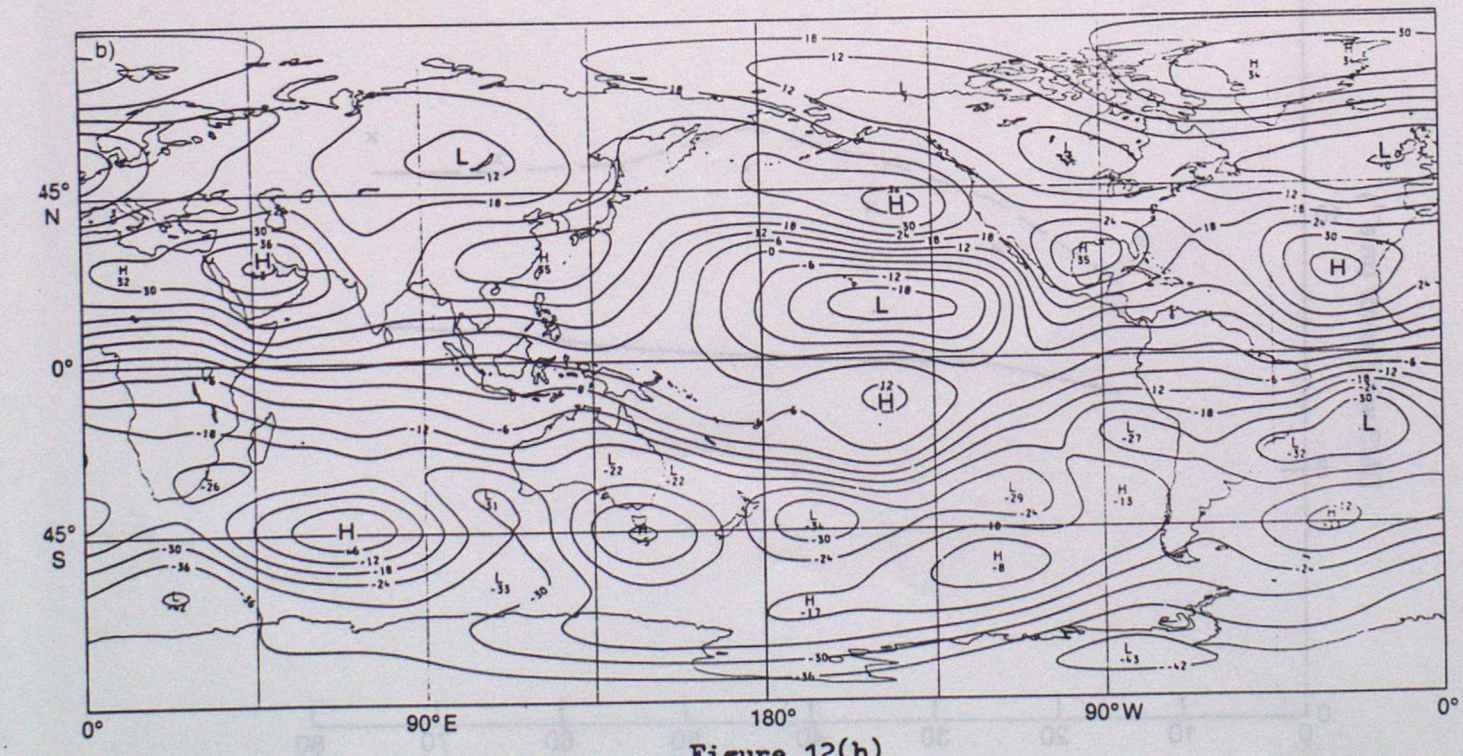

Figure 12(b)

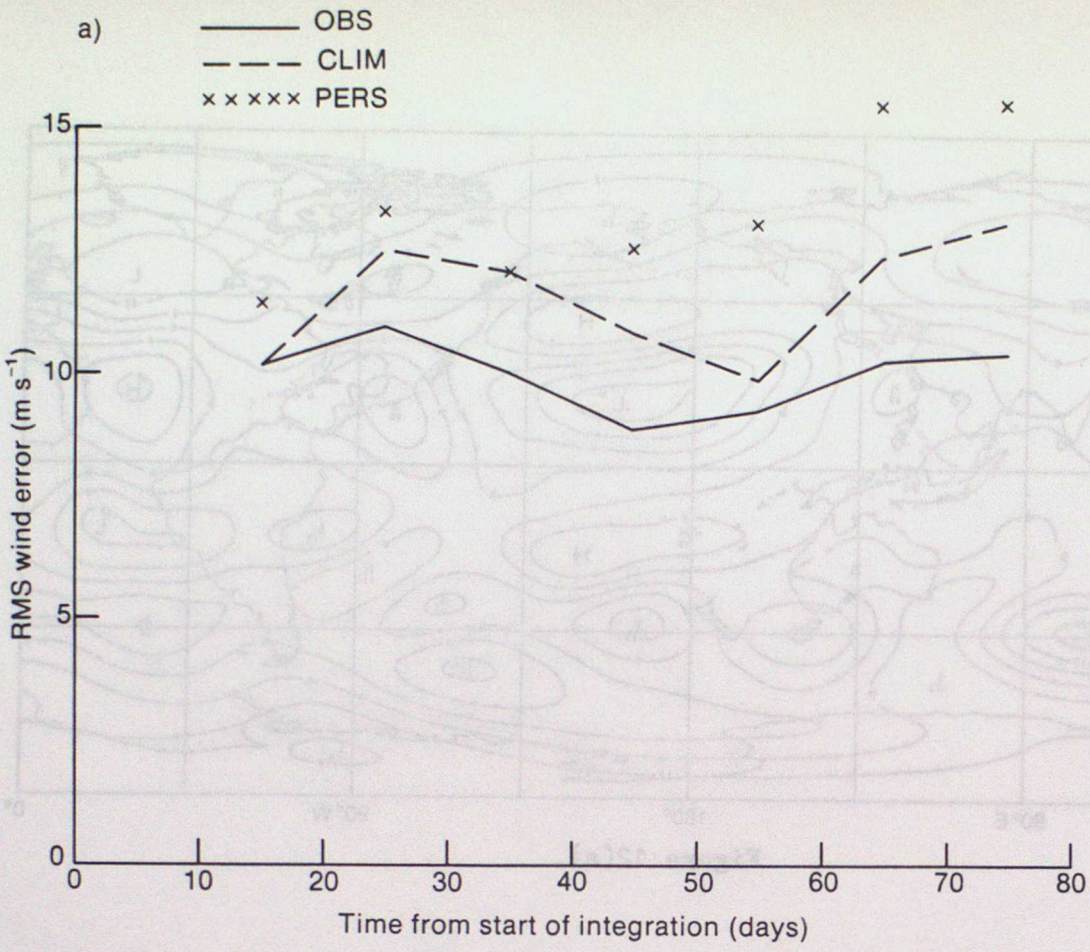

Figure 13(a)

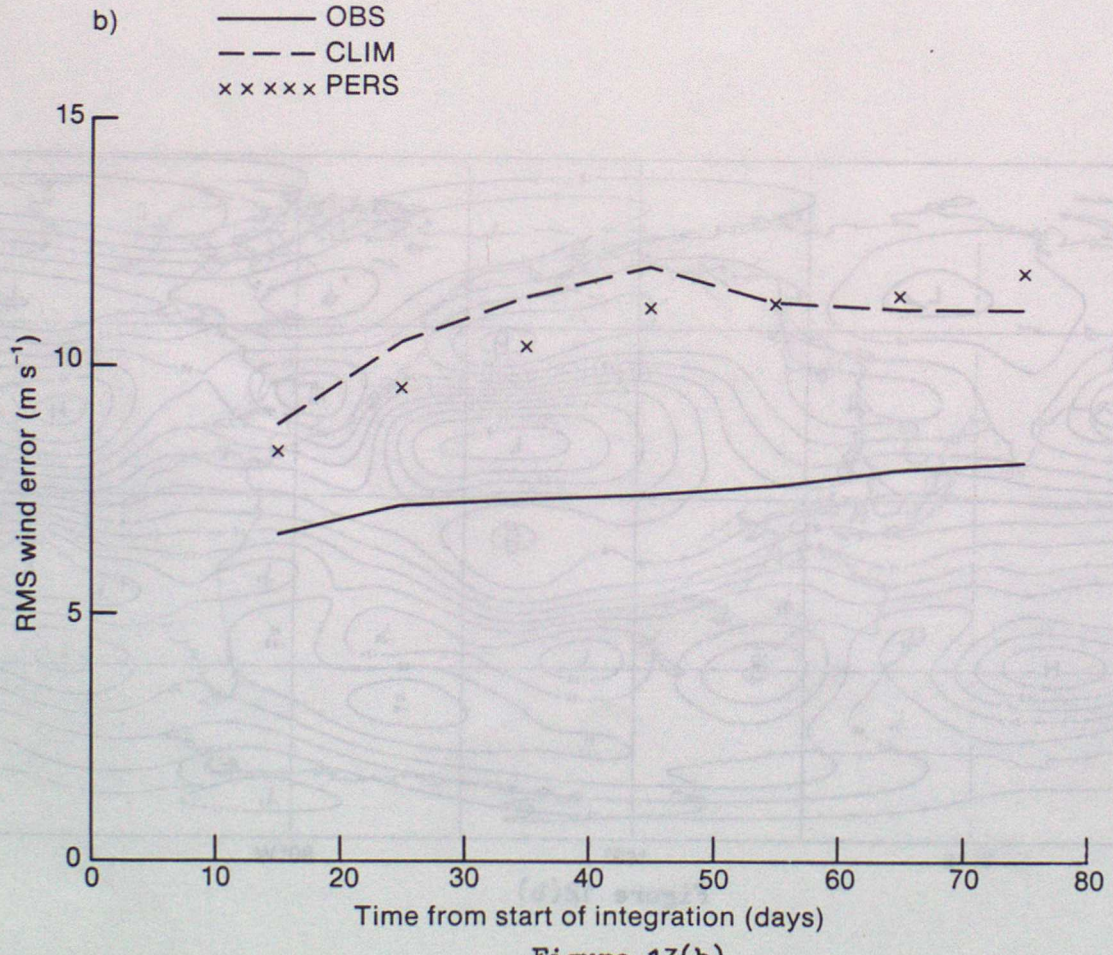

Figure 13(b)

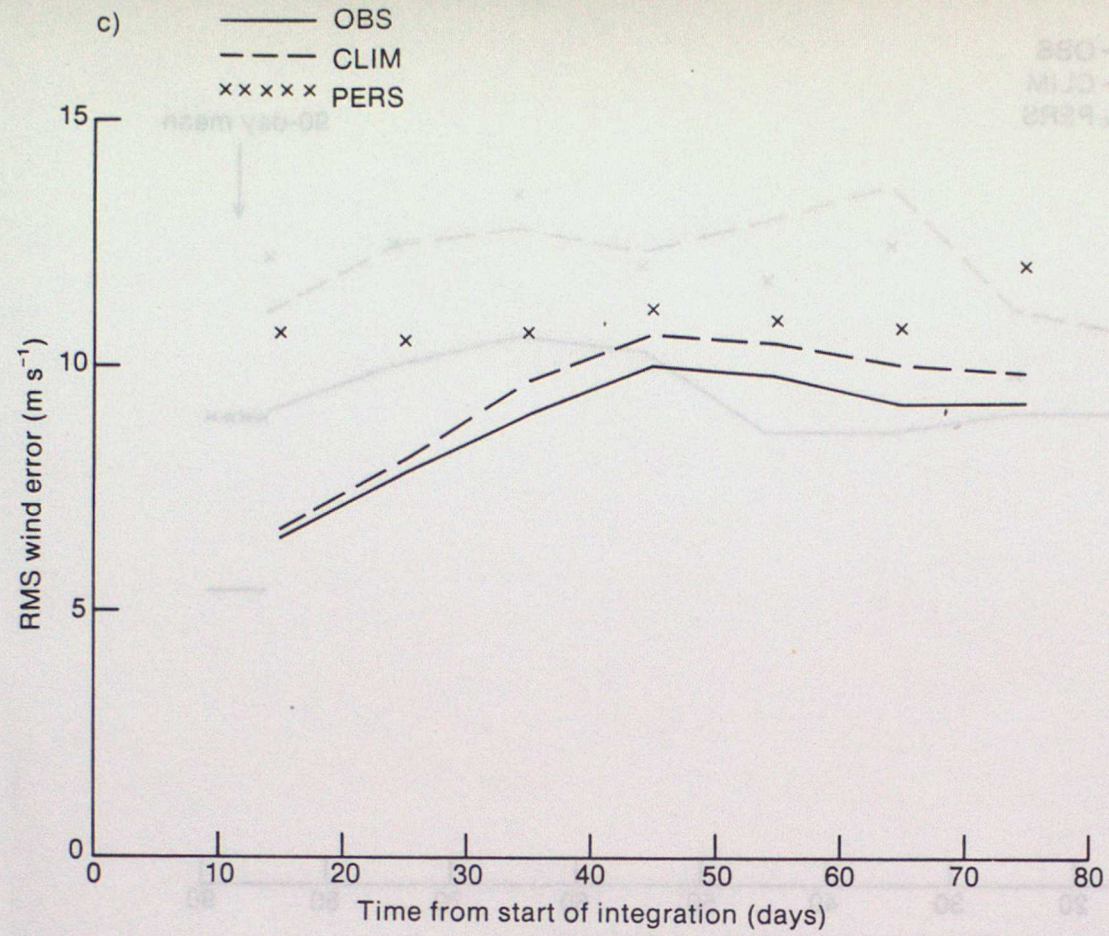

Figure 13(c)

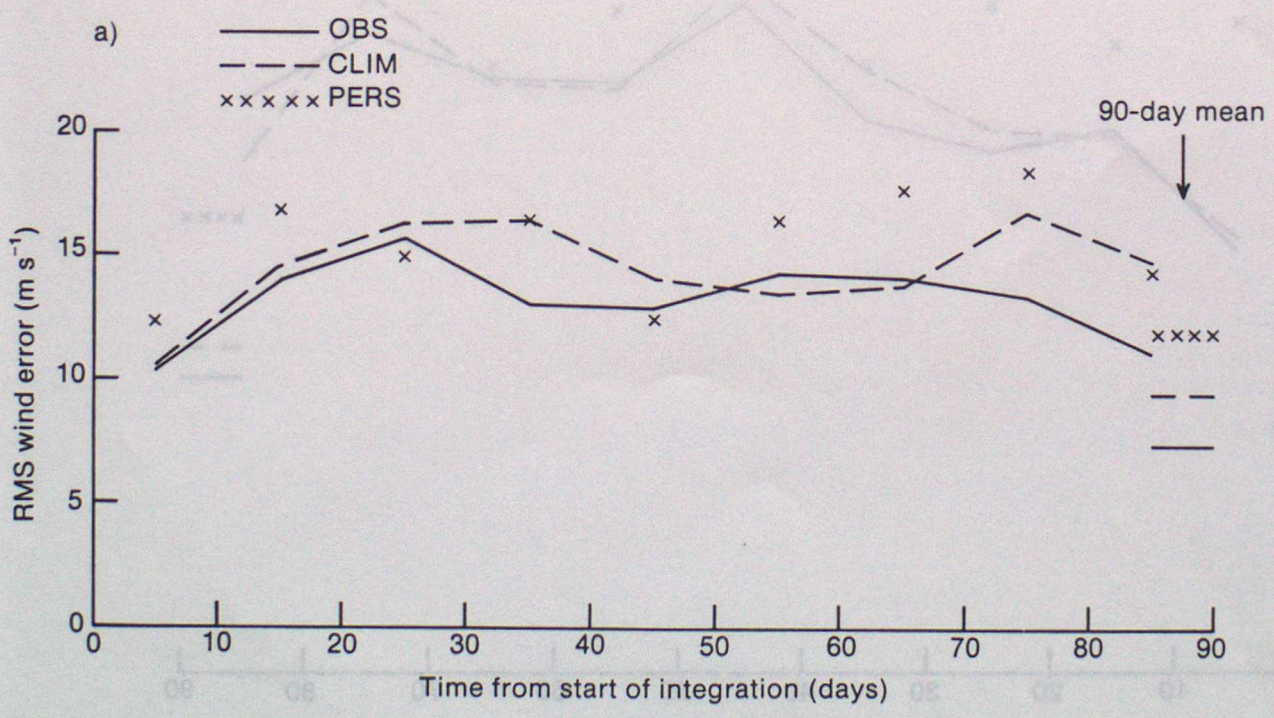

Figure 14(a)

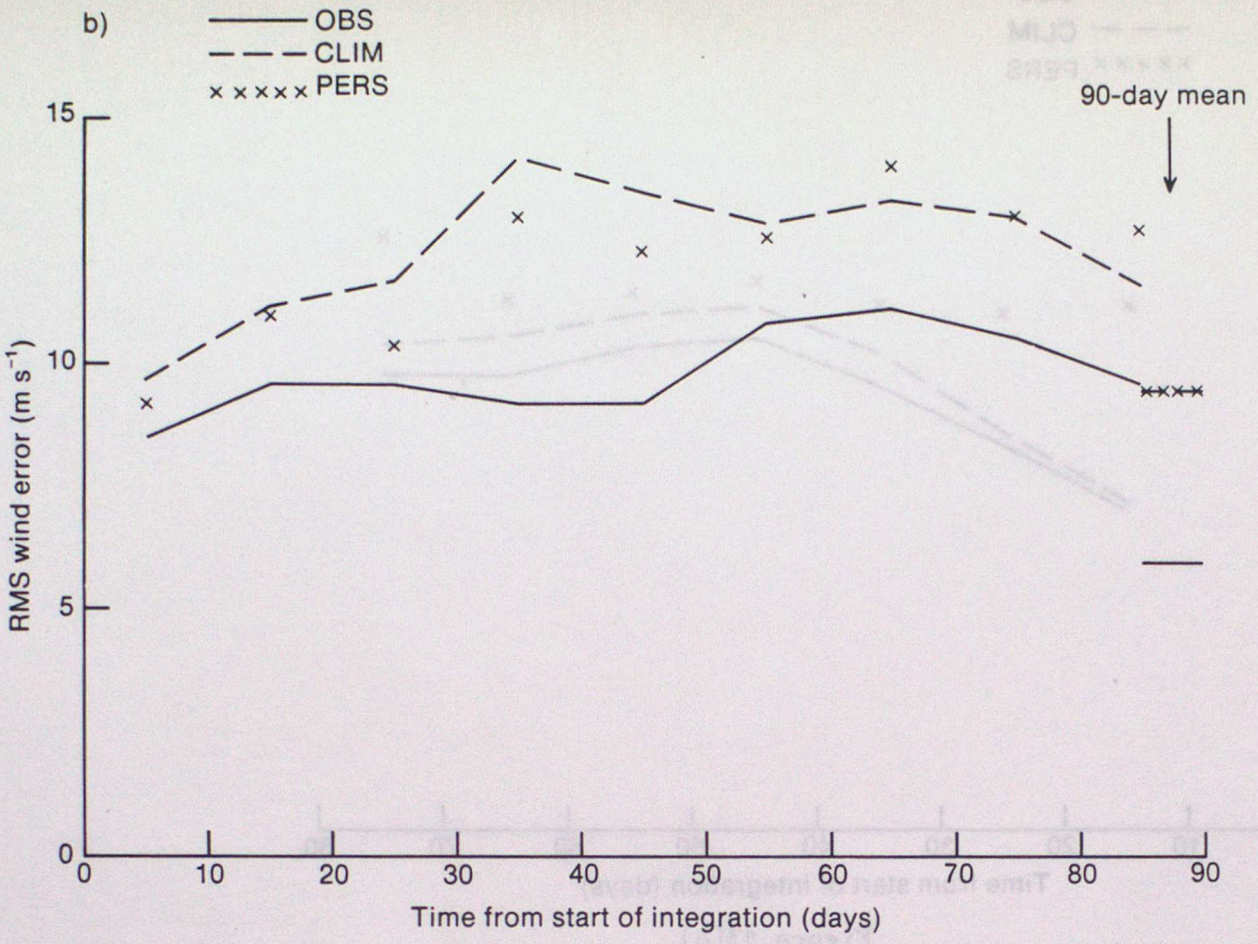

Figure 14(b)

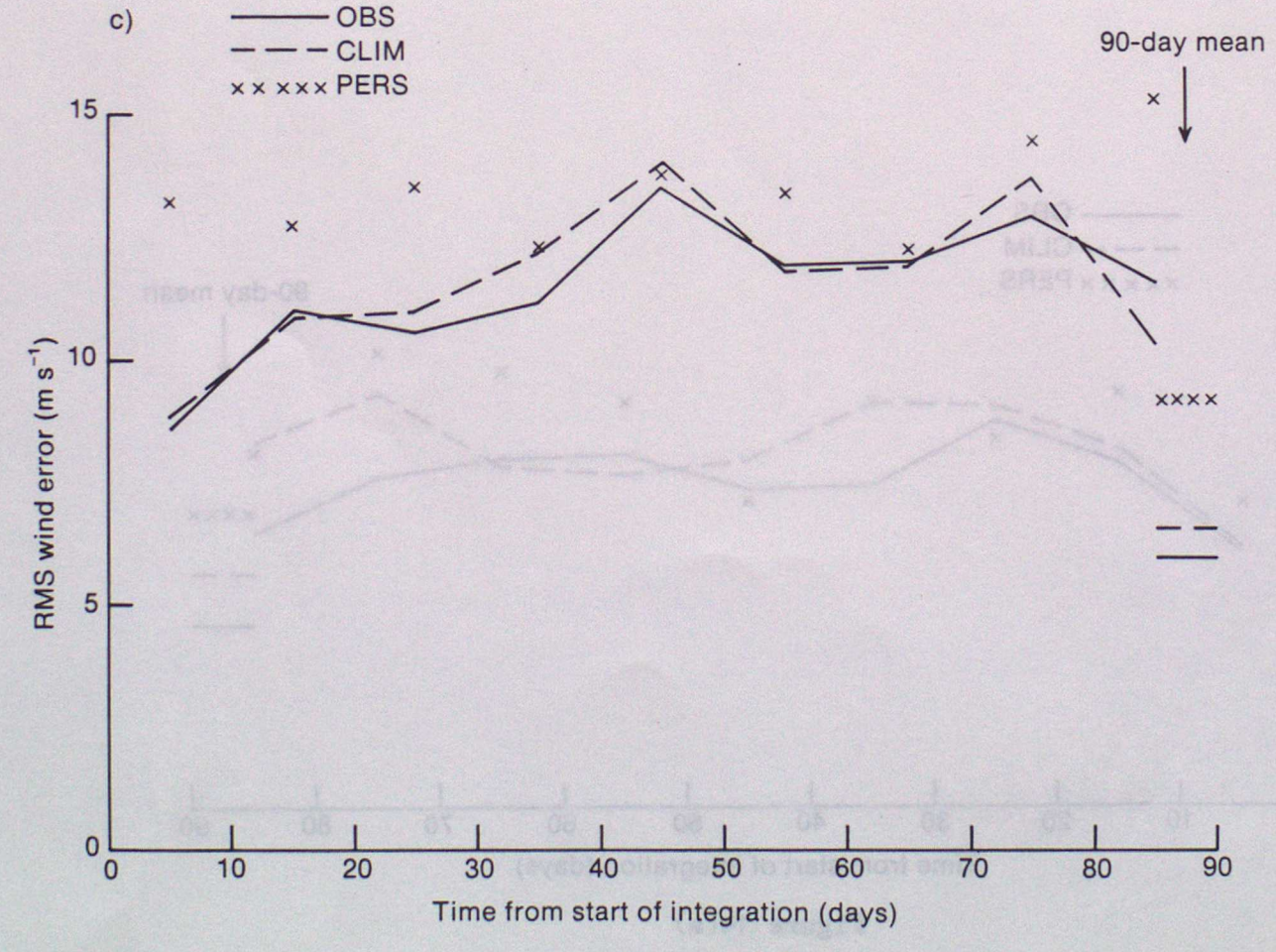

Figure 14(c)

a)

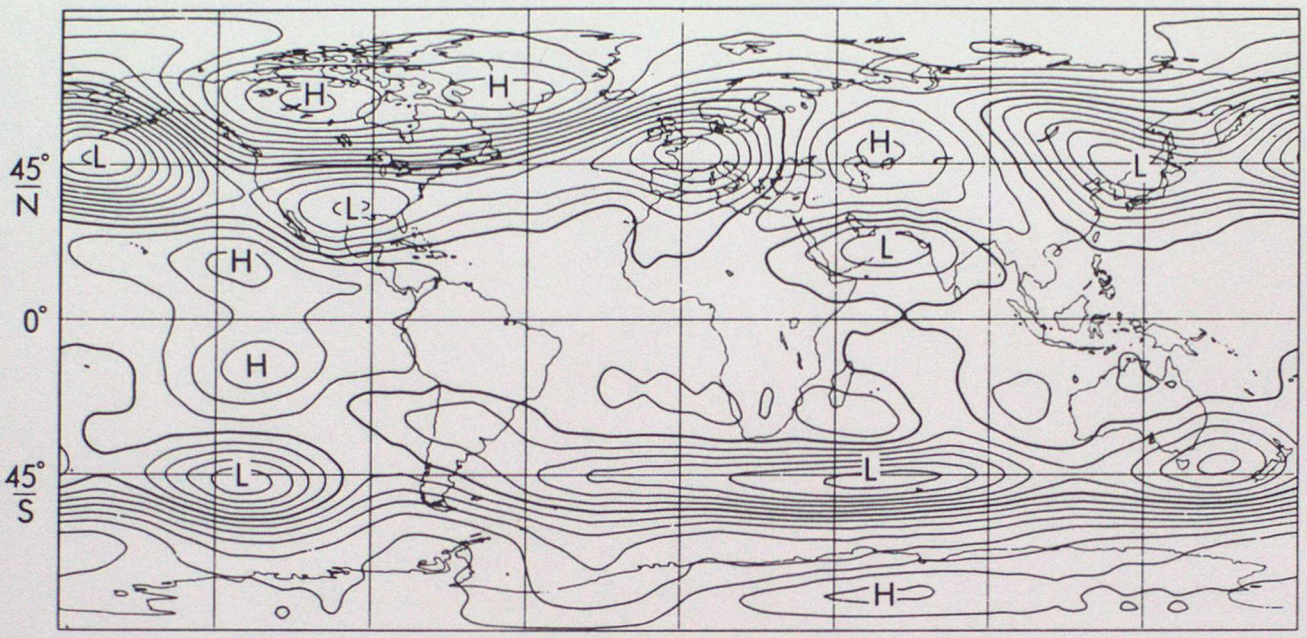

Figure 15(a)

b)

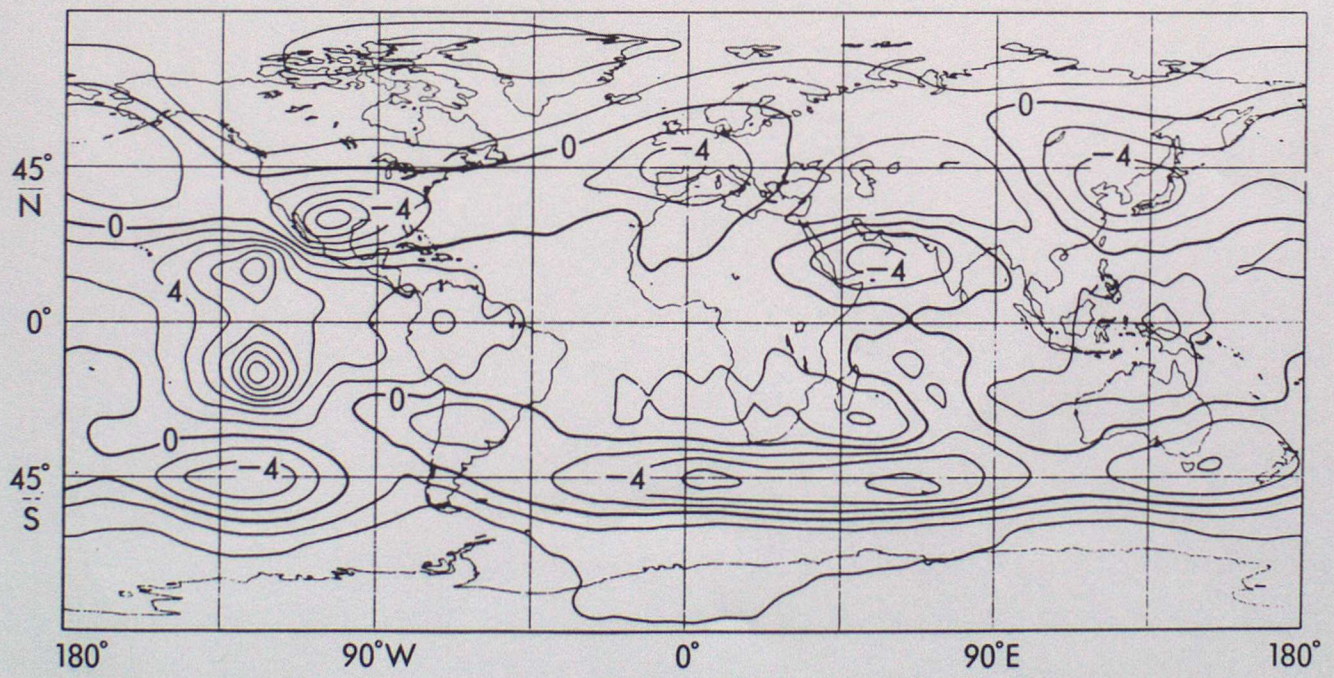

Figure 15(b)

INDEX TO LONG-RANGE FORECASTING AND CLIMATE RESEARCH SERIES

1) THE CLIMATE OF THE WORLD - Introduction and description of world climate.
by C K Folland (March 1986)

2) THE CLIMATE OF THE WORLD - Forcing and feedback processess.
by C K Folland (March 1986)

3) THE CLIMATE OF THE WORLD - El Nino/Southern Oscillation and the Quasi-biennial Oscillation.
by C K Folland (March 1986)

4) THE CLIMATE OF THE WORLD - Climate change: the ancient earth to the 'Little Ice Age'.
by C K Folland (March 1986)

5) THE CLIMATE OF THE WORLD - Climate change: the instrumental period.
by C K Folland (March 1986)

6) THE CLIMATE OF THE WORLD - Carbon dioxide and climate (with appendix on simple climate models).
by C K Folland (March 1986)

7) Sahel rainfall,Northern Hemisphere circulation anomalies and worldwide sea temperature changes. (To be published in the Proceedings of the "Pontifical Academy of Sciences Study Week", Vatican, 23-27 September 1986).
by C K Folland, D E Parker, M N Ward and A W Colman (September 1986)

8) Lagged-average forecast experiments with a 5-level general circulation model.
by J M Murphy (March 1986)

9) Statistical Aspects of Ensemble Forecasts.
by J M Murphy (July 1986)

10) The Impact of El Nino on an Ensemble of Extended-Range Forecasts. (Submitted to Monthly Weather Review)
by J A Owen and T N Palmer (December 1986)